**Atmospheric
Chemistry
and Physics**

# Comparison of CMAM simulations of carbon monoxide (CO), nitrous oxide (N₂O), and methane (CH₄) with observations from Odin/SMR, ACE-FTS, and Aura/MLS

**J. J. Jin[1], K. Semeniuk[1], S. R. Beagley[1], V. I. Fomichev[1], A. I. Jonsson[2], J. C. McConnell[1], J. Urban[3], D. Murtagh[3], G. L. Manney[4,5], C. D. Boone[6], P. F. Bernath[6,7], K. A. Walker[2,6], B. Barret[8], P. Ricaud[8], and E. Dupuy[6]**

[1]Department of Earth and Space Science and Engineering, York University, Toronto, Ontario, Canada
[2]Department of Physics, University of Toronto, Toronto, Ontario, Canada
[3]Department of Radio and Space Science, Chalmers University of Technology, Goteborg, Sweden
[4]Jet Propulsion Laboratory, California Institute of Technology, Pasadena, CA, USA
[5]New Mexico Institute of Mining and Technology, Socorro, NM, USA
[6]Department of Chemistry, University of Waterloo, Waterloo, Ontario, Canada
[7]Department of Chemistry, University of York, Heslington, York, UK
[8]Laboratoire d'Aérologie, UMR 5560 CNRS/Université Paul Sabatier, Observatoire de Midi-Pyrénées, Toulouse, France

**Abstract.** Simulations of CO, N₂O and CH₄ from a coupled chemistry-climate model (CMAM) are compared with satellite measurements from Odin Sub-Millimeter Radiometer (Odin/SMR), Atmospheric Chemistry Experiment Fourier Transform Spectrometer (ACE-FTS), and Aura Microwave Limb Sounder (Aura/MLS). Pressure-latitude cross-sections and seasonal time series demonstrate that CMAM reproduces the observed global CO, N₂O, and CH₄ distributions quite well. Generally, excellent agreement with measurements is found between CO simulations and observations in the stratosphere and mesosphere. Differences between the simulations and the ACE-FTS observations are generally within 30%, and the differences between CMAM results and SMR and MLS observations are slightly larger. These differences are comparable with the difference between the instruments in the upper stratosphere and mesosphere. Comparisons of N₂O show that CMAM results are usually within 15% of the measurements in the lower and middle stratosphere, and the observations are close to each other. However, the standard version of CMAM has a low N₂O bias in the upper stratosphere. The CMAM CH₄ distribution also reproduces the observations in the lower stratosphere, but has a similar but smaller negative bias in the upper stratosphere. The negative bias may be due to that the gravity drag is not fully resolved in the model. The simulated polar CO evolution in the Arctic and Antarctic agrees with the ACE and MLS observations. CO measurements from 2006 show evidence of enhanced descent of air from the mesosphere into the stratosphere in the Arctic after strong stratospheric sudden warmings (SSWs). CMAM also shows strong descent of air after SSWs. In the tropics, CMAM captures the annual oscillation in the lower stratosphere and the semiannual oscillations at the stratopause and mesopause seen in Aura/MLS CO and N₂O observations and in Odin/SMR N₂O observations. The Odin/SMR and Aura/MLS N₂O observations also show a quasi-biennial oscillation (QBO) in the upper stratosphere, whereas, the CMAM does not have QBO included. This study confirms that CMAM is able to simulate middle atmospheric transport processes reasonably well.

## 1 Introduction

The Canadian Middle Atmosphere Model (CMAM) is a coupled Chemistry-Climate Model (CCM) and incorporates a comprehensive representation of middle atmospheric radiation, dynamics, and chemistry as well as standard processes for tropospheric general circulation models (GCMs)

*Correspondence to:* J. J. Jin
(jin@nimbus.yorku.ca)

(Beagley et al., 1997; de Grandpré et al., 2000; Fomichev et al., 2004). The model has been extensively used to investigate middle atmospheric climate change (e.g., Jonsson et al., 2004; Fomichev et al., 2007), conduct data assimilation (Polavarapu et al., 2005), and assess changes to the global ozone layer (WMO, 2003, 2007; Eyring et al., 2006, 2007; Shepherd and Jonsson, 2008). A previous model assessment showed that the model ozone climatology agrees well with observations (de Grandpré et al., 2000). This was also confirmed in a more recent assessment (Eyring et al., 2006) where a limited set of temperature, ozone ($O_3$), water vapour ($H_2O$), methane ($CH_4$) and hydrogen chloride (HCl) measurements and age of air estimates were compared with simulations from over a dozen CCMs. This comparison, which focused on model inter-comparisons rather than on extensive comparisons with measurements, also suggested that CMAM is representative of the better-performing models. In this paper, we perform a much more extensive and challenging comparison of CMAM with measurements. In particular, CMAM results for carbon monoxide (CO), nitrous oxide ($N_2O$) and $CH_4$ are compared with observations from three satellite instruments: Atmospheric Chemistry Experiment Fourier Transform Spectrometer (ACE-FTS) (Bernath et al., 2005), Odin Sub-Millimeter Radiometer (Odin/SMR, herein SMR) (Murtagh et al., 2002), and Aura Microwave Limb Sounder (Aura/MLS, herein MLS) (Waters et al., 2006).

CO, $N_2O$ and $CH_4$ have local chemical lifetimes in the middle atmosphere that are equivalent to or longer than the typical advection and mixing timescales, and thus they act as tracers for middle atmospheric transport processes (e.g., Brasseur and Solomon, 2005). CO in the middle atmosphere is mainly produced by oxidation of $CH_4$ in the stratosphere and by photolysis of $CO_2$ in the mesosphere and thermosphere, and is mainly destroyed through the reaction with hydroxyl radicals (OH). The local chemical lifetime of CO is about six months in the lower stratosphere and three weeks in the upper stratosphere. It increases to about two months in the lower mesosphere. In the upper mesosphere the local lifetime can be over one year and becomes even longer in the thermosphere. In addition, there is virtually no chemical loss during polar night because of the absence of OH in regions without sunlight. $N_2O$ is emitted at the surface of the Earth and its local chemical lifetime varies from years in the lower stratosphere to weeks in the upper stratosphere and mesosphere. $N_2O$ is primarily destroyed by photolysis; however, the oxidation of $N_2O$ through the reaction with excited oxygen atoms ($O(^1D)$) is the main source of stratospheric nitrogen oxides ($NO_x=NO+NO_2$). $CH_4$ is also emitted at the Earth's surface and is destroyed through reactions with OH and $O(^1D)$ producing CO and $H_2O$ in the middle atmosphere. It also reacts with atomic chlorine to produce HCl. $CH_4$ has a local chemical lifetime ranging from over 100 years in the lower stratosphere to months in the middle stratosphere. Its lifetime increases to a few years at the stratopause, but decreases again above that, ranging from weeks to days above

70 km due to photolysis, principally by Lyman-$\alpha$ radiation. Due to the different sources of origin for the different species and their different local lifetimes in the middle atmosphere their spatial distributions are distinctly different. As $N_2O$ and $CH_4$ are transported from the surface their volume mixing ratios (VMRs) decrease with height. For CO, which primarily is produced locally within the middle atmosphere, the VMR generally increases with height. As a result, these three species allow us to test different dynamical aspects of the model.

The SMR on board the Odin satellite performs limb observations of trace gases in the spectral range 486–581 GHz (Murtagh et al., 2002). CO is retrieved from the 576.6 GHz band between ~18–100 km with an altitude resolution of about 3 km. The retrieval methodology for CO is described by Dupuy et al. (2004). $N_2O$ is retrieved from a line at 502.3 GHz in the altitude range 13–50 km with a vertical resolution of 1.5–2 km (Urban et al., 2005, 2006). ACE-FTS is a Fourier Transform Spectrometer on the Canadian Atmospheric Chemistry Experiment (ACE) satellite SCISAT–1 (Bernath et al., 2005). It currently measures temperature, pressure and more than thirty species involved in ozone-related chemistry as well as isotopologues of some of the molecules. ACE-FTS observes solar occultations in the spectral range 750–4400 cm$^{-1}$ (2.3–13.3 $\mu$m) with a high spectral resolution of 0.02 cm$^{-1}$. The vertical resolution is ~3–4 km. The retrieval approach for temperature, pressure, and volume mixing ratios is described by Boone et al. (2005). Information on the CO retrievals can also be found in Clerbaux et al. (2005). We also compare the model simulations with measurements from the MLS (Waters et al., 2006) on the Aura satellite. The MLS CO data are retrieved from the measurements of the 240 GHz radiometer with a vertical resolution of about 2.5 km in the stratosphere and mesosphere and about 4 km in the upper troposphere and lower stratosphere (Pumphrey et al., 2007; Livesey et al., 2008). The $N_2O$ measurements are derived from the 640 GHz retrievals with a vertical resolution of about 4–5 km between 100–1 hPa (Lambert et al., 2007).

The three different instruments provide datasets with different properties: ACE-FTS observations provide precise measurements but its spatial coverage is limited, especially at low latitudes. MLS measurements provide a good global coverage and the SMR observations not only have a global coverage but also a longer time record. Recent comparisons between the three instruments show that the measurements of CO, $N_2O$ and $CH_4$ are reliable (Barret et al., 2006; Clerbaux et al., 2008; De Mazière et al., 2008; Lambert et al., 2007; Livesey et al., 2008; Pumphrey et al., 2007; Strong et al., 2008). The difference between ACE-FTS and SMR CO measurements is less than 25% between 25–68 km, and ACE-FTS CO is about 50% lower than the CO from SMR below 22 km. Compared with MLS, the ACE-FTS CO is significantly lower in the troposphere, up to 50% higher in the lower stratosphere, and about 25% lower in the mesosphere.

MLS CO is noisier than CO from ACE-FTS and SMR (Clerbaux et al., 2008; Pumphrey et al., 2007). The MLS $N_2O$ measurements are close to the ACE-FTS and SMR data, generally within 5–10% between 100–1 hPa (Strong et al., 2008). The agreement between ACE-FTS and SMR $N_2O$ measurements is also excellent below 40 km where the difference is generally less than 10% on average. At 40 km, the relative agreement becomes worse because of the small $N_2O$ mixing ratios there, but the absolute difference is small, about of 2–3 ppbv (Lambert et al., 2007; Strong et al., 2008). De Mazière et al. (2008) show that the ACE-FTS $CH_4$ also has a generally good agreement with other observations but has a 5–20% positive bias between 10 and 55 km compared to measurements from the Halogen Occultation Experiment (HALOE) on board the Upper Atmosphere Research Satellite (UARS).

An earlier inter-comparison of CO showed good agreement between ACE-FTS and SMR at various latitudes and seasons, and good agreement between these measurements and CMAM simulations at low latitudes as well as poor agreement between the measurements and model results in the polar winter stratosphere (Jin et al., 2005). The poor agreement was related to the abnormal meteorological conditions for the Arctic winter 2004 (Manney et al., 2005) and the large background vertical diffusion coefficient used in the model at that time. That coefficient has now been reduced and the model's performance has generally improved, particularly in the lower and middle stratosphere. Hence a new and more detailed study is motivated.

In Sect. 2, the CMAM simulation and the processing of the various datasets are described. The comparisons of CO, $N_2O$, and $CH_4$ are presented in Sects. 3, 4 and 5, respectively. The time evolution of the measurements and the model results in the polar regions are analyzed in Sect. 6. The enhanced Arctic upper stratosphere and lower mesosphere descent associated with stratospheric sudden warmings in 2006, which has been highlighted in recent studies (Randall et al., 2006; Manney et al., 2008a, b), is also discussed in this section. To our knowledge this is the first time that the complete annual evolution of CO in the stratosphere and mesosphere in the Arctic and Antarctic is shown. In Sect. 7, the annual and inter-annual oscillations in the measurements and the model simulation in the tropics are compared. Section 8 provides a summary of this study.

## 2 CMAM simulation and measurement

This study uses the standard version of CMAM which has a spectral horizontal resolution of T31 with an associated horizontal grid of 64×32 points (5.8°×5.8°). There are 71 vertical levels and the upper boundary is at $6 \times 10^{-4}$ hPa (~95 km geometric altitude). The standard version of the model includes comprehensive stratospheric gas phase and heterogeneous chemistry, but tropospheric chemistry is limited and

detailed surface emissions are not included in the model. Additional details are given in de Grandpré et al. (2000). Details of the particular simulation used for the comparisons herein are given in Eyring et al. (2006). Surface concentrations of greenhouse gases $CO_2$, $CH_4$ and $N_2O$ are based on observations and scenarios from the Intergovernmental Panel on Climate Change (IPCC) (2001) and surface concentrations of ozone depleting substances are in accordance with WMO (2003). No treatments of solar variability or volcanic activity are included and the quasi-biennial oscillation in the tropical stratospheric zonal wind is neither internally generated nor externally driven. Model results for the period of 2004–2007 are used in this study.

For comparison, the ACE-FTS, SMR and MLS retrievals are first binned into latitudinal bands centered on the CMAM grid and interpolated to the CMAM pressure levels. Monthly zonal averages are calculated from the binned datasets. In order to reduce the noise in the SMR and MLS CO retrievals, however, running averages in 10 degree-wide latitude bands, centered at the CMAM latitude grid points are used (Fig. 1). For ACE-FTS, version 2.2 retrievals for the period February 2004 to August 2007 are used. Validation studies, including the works introduced in Sect. 1, can be found in the special issue on "Validation results for the Atmospheric Chemistry Experiment" in Atmospheric Chemistry and Physics (2008). The observational geometry of the ACE-FTS instrument is such that up to 15 sunrise and 15 sunset observations are collected along two latitude circles per day. One of the circles is in the Northern Hemisphere and the other is in the Southern Hemisphere. The observed latitudes vary with time so that over several months global coverage is achieved. We note that this distribution of occultations means that the temporal coverage for some latitude bins and months is limited. As a result, only the CMAM zonal means sampled at the nearest latitudes to the ACE-FTS locations on the simulation day are applied in calculating the relative differences ACE-FTS/CMAM in Sects. 3, 4, and 5.

SMR and MLS both provide measurements with near-global coverage, between 82.5° S and 82.5° N. The observation time for SMR was divided between aeronomy and astronomy, but the astronomical observations ceased in April 2007 and the SMR is now used solely for aeronomical observations. For SMR, the results from the latest CO retrievals, version-225, between October 2003 and August 2006, and the version 2.1 $N_2O$ between July 2001 and February 2007 are used. In contrast to $N_2O$, CO measurements are conducted only on about 1–2 days per month (see Table 1), which likely introduces biases in the derived monthly averages compared to mean atmospheric conditions. However, we estimate that this error is small considering the long local chemical lifetime of CO in the atmosphere, as noted above, except at the middle and polar latitudes where fast meridional and vertical transport affects the CO distribution in winter.

For MLS, we use the version 2.2 retrievals between August 2004 and April 2008. Information on the processing and

**Table 1.** Availability of SMR v225 CO data given by date ranges for each month and year.

| Year | Jan | Feb | Mar | Apr | May | Jun | Jul | Aug | Sep | Oct | Nov | Dec |
|---|---|---|---|---|---|---|---|---|---|---|---|---|
| 2003 | | | | | | | | | | 8–9 | 13–14; 30 | 1; 19–20 |
| 2004 | 10–11; 29–30 | 15–16 | 5–6; 22–23 | 27–28 | 16–17 | 21–22 | 27–28 | 13–14; 19–20; 25–26 | 1–2; 18–19 | | 29–30 | |
| 2005 | | | 23–24 | | | | | | | | | |
| 2006 | 13–18; 21–22; 24–25; 27–28; 30–31 | 1–2 | | | | | | 31 | | | | |

validation of this new version of the data can be found in a special section on Aura Validation in Journal of Geophysical Research, Vol. 112(D24), 2007.

## 3   CO comparisons

Figure 1 shows monthly and zonal mean CO latitude-pressure cross-sections of the model simulation and the observations above 400 hPa for April and July. Since the SMR observations currently are available only for limited time periods (particularly during 2004, see Table 1), we use data from April 2004 and July 2004 for the SMR monthly averages in April and July, respectively. However, all other monthly means for observations and the model simulation are multi-year averages. As will be shown in the paper, the CMAM can reproduce the measurements in the stratosphere and mesosphere quite well.

The model simulation and the observations show large and comparable CO mixing ratios in the mesosphere. The CO mixing ratio generally increases from ∼0.1 ppmv in the lower mesosphere to about 10–50 ppmv in the upper mesosphere. This strong increase with altitude is caused by increasing photolysis of $CO_2$ with altitude, and the relatively constant or increasing local chemical lifetime for the loss reaction with OH. In July, there is also a strong meridional gradient from the northern polar region to the southern polar region in the mesosphere, reflecting the meridional circulation from the summer hemisphere to the winter hemisphere in the mesosphere, with ascent over the summer pole and descent over the winter pole (Andrews et al., 1987).

A downward extension of the high mesospheric CO values into the upper stratosphere at the southern high latitudes in July is evident both in the CMAM results and in the ACE-FTS, SMR and MLS observations. The 0.1 ppmv contour in CMAM, SMR, and MLS data descends from about 0.5 hPa (∼53 km) in April to about 7 hPa (∼35 km) in July, which corresponds to a descent rate of about 6 km per month. A strong CO meridional gradient in the winter polar region and associated downward transport have been reported in observations by ISAMS (Allen et al., 2000), SMR (Dupuy et al., 2004) and MLS (Pumphrey et al., 2007). The ISAMS observations showed a similar descent rate in the Antarctic upper stratosphere and lower mesosphere from late April to late July (Fig. 1 in Allen et al., 2000). In the upper stratosphere and lower mesosphere, the ACE-FTS shows an opposite meridional gradient to the gradient in the CMAM simulation and the SMR and MLS observations between 60° S and 90° S in April. This difference is because the ACE-FTS sample locations move towards the sub-polar region during this period of fast descent (see Fig. 9 in Sect. 6).

The observed enhancement of CO in the middle and upper stratosphere between 10 hPa and 1 hPa (∼32 km and 50 km) in the tropics is due to $CH_4$ oxidation in rising air in this region (Allen et al., 1999) and is clearly captured by the model. The enhancement displays a seasonal variation in the model simulation between 5 hPa and 1 hPa (∼38 km and 50 km), being notably weaker in solstice seasons (i.e., in July) than in equinox seasons (i.e., in April). This is due to the Semiannual Oscillation (SAO), which will be discussed in Sect. 7. Briefly, the CO variation is caused by a combination of upward transport of $CH_4$ and its oxidation. However, it is difficult to see the seasonal variation in the measurements due to the discontinuous record of the ACE-FTS tropical retrievals and due to the noise in the SMR and MLS data.

The CMAM produces very small CO mixing ratios (less than 15 ppbv) around 5 hPa in the Antarctic middle stratosphere in April, and in the lower tropical stratosphere (around 50 hPa, 20 km) in April and in July. These small CO values are also observed by the satellite instruments although SMR and MLS are somewhat noisier than ACE-FTS. The polar minimum is due to the combination of chemical loss by OH and reduced meridional transport from lower latitudes. The minimum in the tropical lower stratosphere represents the transition region between two mechanisms for
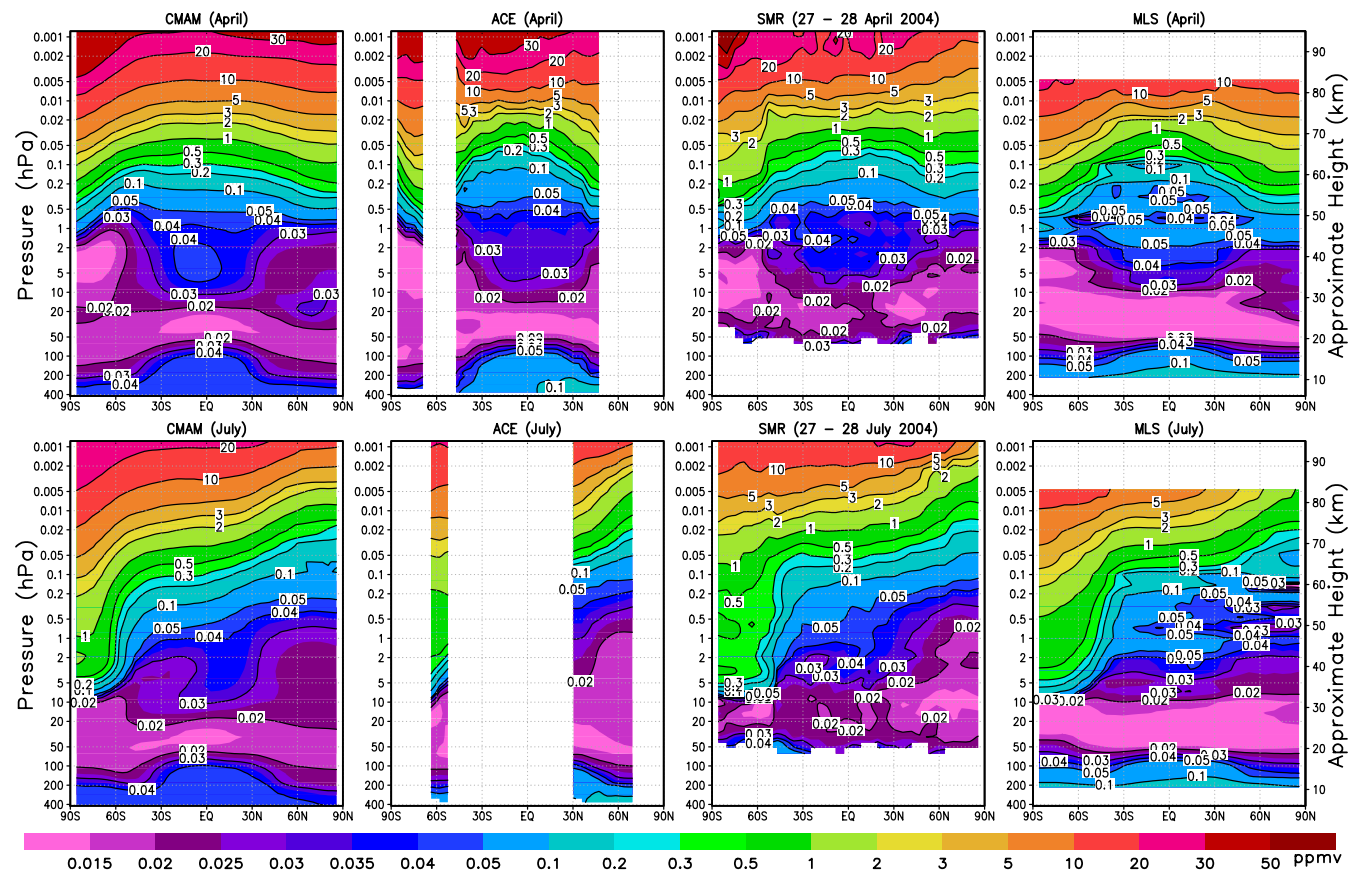
**Fig. 1.** Monthly zonal mean latitude-pressure cross-sections of CO from CMAM (January 2004–December 2007), ACE-FTS (February 2004–August 2008), SMR (April 2004 and July 2004), and MLS (August 2004–April 2008). 10-degree latitude running average is used in SMR and MLS zonal means shown in here.

CO production: fossil fuel and biomass burning in the troposphere and chemical production from $CH_4$ in the stratosphere. In addition, MLS has a significant negative bias in the lower stratosphere (around 30 hPa) (Pumphrey et al., 2007), which will be shown more clearly in Fig. 2.

Figure 2 shows the ratios of the observations to the CMAM simulation for monthly mean profiles at 74.8° S in September, 41.5° S in January, 2.8° S in April, 36.6° N in July and 74.8° N in October. The relative differences between the observations and the simulation vary significantly in the vertical, but the ratios ACE-FTS/CMAM are mostly within 0.7–1.3 in the stratosphere and mesosphere, which is consistent with the good agreement shown in the pressure-latitude cross-sections (Fig. 1). The ratios SMR/CMAM are close to the ratios ACE-FTS/CMAM at lower and middle latitudes but are smaller than the latter at high latitudes. Although the ratios MLS/CMAM are noisy, they generally follow the ratios ACE-FTS/CMAM and SMR/CMAM. We note that CMAM has a positive bias by a factor of two between 0.5 hPa and 0.02 hPa (about 53 km–75 km) in the tropics, which is

due to the slow vertical diffusion in the lower mesosphere (see Sects. 4 and 5). Between 10 hPa and 1 hPa, CMAM is close to ACE-FTS and SMR at the middle and lower latitudes. However, the CMAM values are larger than the ACE-FTS and SMR observations at 74.8° S in September by a factor of two, which is due to a stronger Antarctic vortex in the model than in the real atmosphere for the years studied. Between 100 hPa and 10 hPa, the CMAM results are close to the ACE-FTS measurements and the difference is usually less than 30%. We note that the ratios MLS/CMAM are extremely small at around 30 hPa, which is due to the significant negative bias of MLS in the lower stratosphere (Pumphrey et al., 2007).

In the upper troposphere (above 300 hPa), CMAM values are similar to ACE-FTS values in the southern polar region, but are much smaller than those from ACE-FTS values at other latitudes, particularly in the Northern Hemisphere. The ratios ACE-FTS/CMAM are less than two at low and middle latitudes and up to about three in the northern polar region. The ratios MLS/CMAM can be as large as three to four
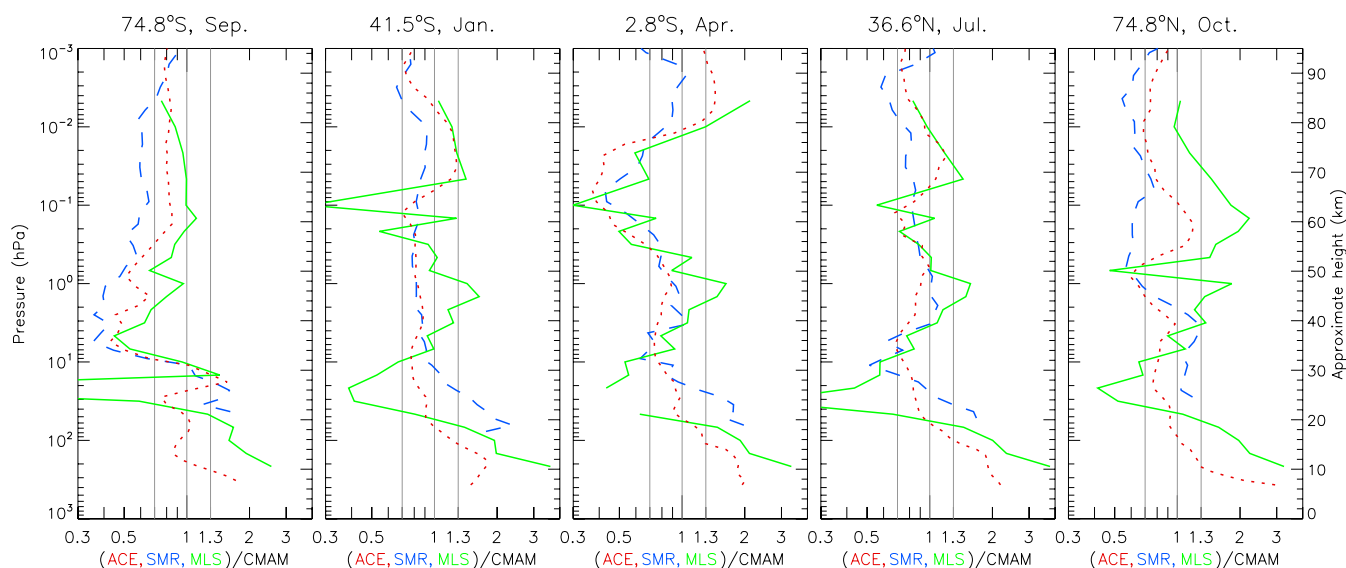
**Fig. 2.** Ratios for monthly mean CO at various latitudes. Blue dashed line, SMR/CMAM; green solid line, MLS/CMAM; red dotted line, ACE-FTS/(CMAM at the ACE-FTS latitudes). The grey vertical straight lines indicate ratios 0.7, 1.0 and 1.3. The CO VMRs are shown in Fig. 1.

at about 200 hPa. However, we note that CMAM does not include detailed tropospheric surface emissions, nor does it include a chemical source from non-methane hydrocarbons: the only tropospheric CO source is from $CH_4$ oxidation. Furthermore, the CMAM CO surface boundary condition used for this simulation is set to a constant value of 50 ppbv, which is far from the real surface values varying from a minimum 35–45 ppbv in the southern summer to a maximum 200–210 ppbv in the northern winter (Brasseur and Solomon, 2005). The large negative biases in CMAM suggest detailed biomass burning emission should be included in order to better simulate the tropospheric CO.

## 4   N$_2$O comparisons

Figure 3 shows the monthly zonal mean latitude-pressure cross-sections of $N_2O$ from CMAM, ACE-FTS, SMR, and MLS for April and July. The distribution of $N_2O$ from the model is quite similar to the observations in the stratosphere below 1 hPa ($\sim$50 km). The values range from over 300 ppbv in the lower stratosphere to less than 1 ppbv in the upper stratosphere. An enhancement is evident in the tropics in both the model results and measurements for all seasons, reflecting persistent upwelling. In addition, the values of the simulation and the observations are similar except that MLS is slightly smaller in the lower tropical stratosphere. In April, both the simulation and observations display small $N_2O$ VMRs in the Antarctic upper stratosphere, which can be attributed to descent in the upper stratosphere from summer to fall (e.g., Randel et al., 1998; Juckes, 2007). In the winter hemisphere sub-tropics and sub-polar regions CMAM

exhibits "mixing barriers" (seen as closely spaced contours, which indicate strong horizontal gradients, in July) (Plumb, 2002) and similar features are observed by SMR, MLS and ACE-FTS.

The CMAM simulation shows two maxima above 5 hPa in April. These two peaks are located at middle latitudes producing a trough in the tropics. ACE-FTS, SMR and MLS similarly show two peaks in the sub-tropics above 5 hPa and the double-peak feature is also present in $CH_4$ measurements (see Fig. 5 and Sect. 5). This feature results from the downward movement associated with the westerly shear of the dynamical SAO at the equator and upward movement in the subtropics (Gray and Pyle, 1986). The double-peak feature also shows a quasi-biennial oscillation. That is, it occurs about every other year in the measurements (Randel et al., 1998). In October, the multi-year averaged observations do not show such a double-peak feature (not shown). However, this feature is seen in every other October but it is weaker than the feature in April and they occur in different calendar years.

Comparison of the observations from each instrument indicates that their distributions are quite similar. However, SMR and MLS measurements have positive biases relative to ACE-FTS above about 10 hPa ($\sim$35 km) at high latitudes in the fall season (in the Antarctic in April and in the Arctic in October). In addition, MLS VMRs rarely exceed 300 ppbv in the tropical lower stratosphere (below 50 hPa), showing a negative bias compared with ACE-FTS and SMR (Lambert et al., 2007).

The ratios of observations to model results (Fig. 4) show varying levels of agreement. There is excellent agreement
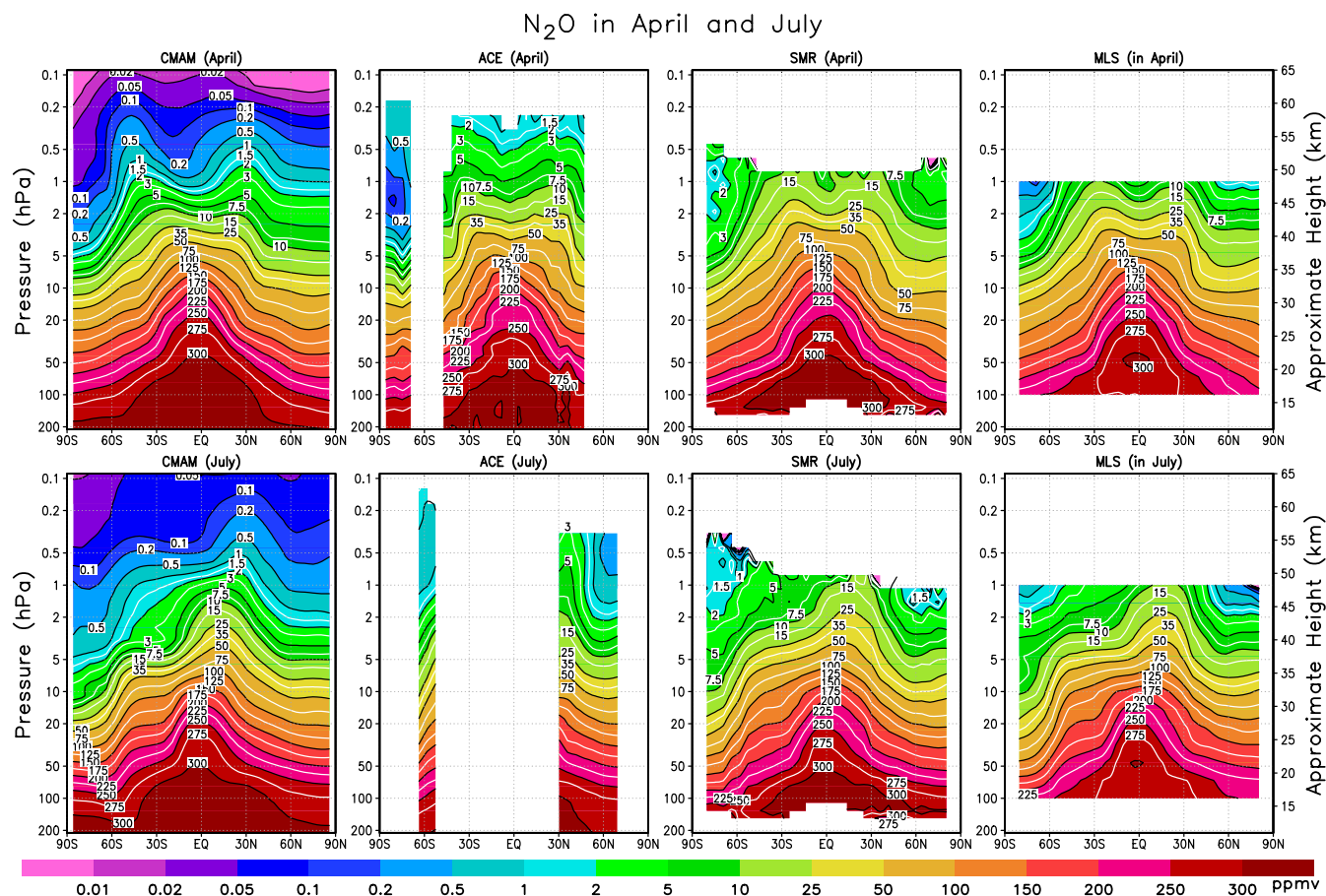
**Fig. 3.** Monthly zonal mean latitude-pressure cross-sections of N$_2$O from CMAM (January 2004–December 2007), ACE-FTS (February 2004–August 2008), SMR (July 2001–February 2007), and MLS (August 2004–April 2008).

between the model results and the observations in the lower and middle stratosphere. In the tropics, the ratios are within 0.85∼1.15 below about 5 hPa (∼38 km) in April. At high latitudes, the same degree of agreement is only achieved at lower altitudes, below 30 hPa (∼25 km) in the Antarctic in September and below 15 hPa (30 km) in the Arctic in October. Above these altitudes, the ratios deviate from unity and increase greatly. The maxima of the ratios vary from 3 to 10 at various latitudes throughout the seasons, indicating that CMAM results are significantly smaller than the measurements, certainly outside the error of the observations. A test of eddy diffusion for tracers associated with non-orographic gravity wave drag (GWD) in CMAM suggests that an increase in the vertical diffusion for chemical tracers, using the GWD scheme, would improve the agreement with the measurements in the middle and upper stratosphere. However, other tests show, when the vertical diffusion in these schemes is turned off, that different GWD schemes have significantly different and strong impact on the vertical distribution of chemical species at the stratopause. That suggests the vertical advection induced by GWD is important for the vertical transport.

## 5 CH$_4$ comparisons

In this section modeled and measured CH$_4$ profiles are compared. Unlike CO and N$_2$O, CH$_4$ is not measured by the SMR or MLS instruments and our comparison is only with ACE-FTS. The monthly zonal mean cross-sections for April and July are shown in Fig. 5, while the ratios ACE-FTS/CMAM are shown in Fig. 6.

It can be seen from Fig. 5 that the CMAM CH$_4$ is quite close to the ACE-FTS observations in the stratosphere (below ∼1 hPa). Both the model results and the observations show the tropical peak attributable to the continuous tropical upwelling (e.g., Plumb, 2002; Shepherd, 2007) and small VMRs in the Antarctic upper stratosphere in April due to the descent in the upper stratosphere from summer to fall (Randel et al., 1998; Juckes, 2007). For CMAM the VMRs decrease in the lower stratosphere from April to July due to the descent within the winter polar vortex. Figure 5 shows that the simulated values are close to the observations below about 1 hPa. Above 1 hPa, however, CMAM is generally smaller except at southern high latitudes in January.
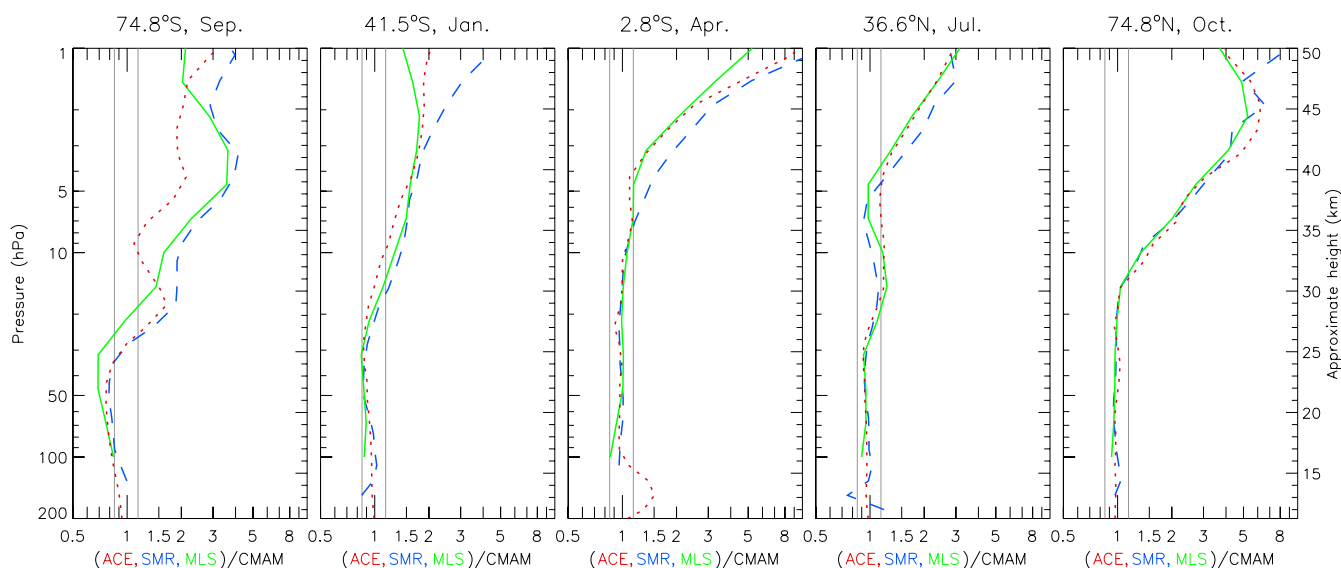
**Fig. 4.** Ratios for monthly mean $N_2O$ profiles at various latitudes. Blue dashed line, SMR/CMAM; green solid line, MLS/CMAM; red dotted line, ACE-FTS/(CMAM at the ACE-FTS latitudes). The grey vertical straight lines indicate ratios 0.85 and 1.15. The VMRs are shown in Fig. 3.
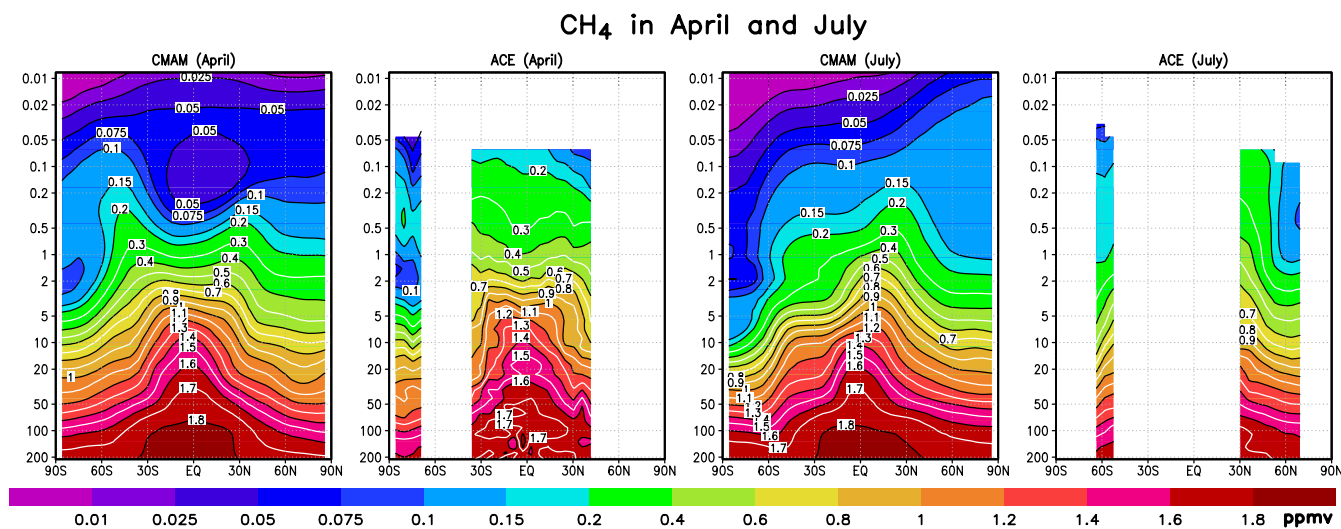


**Fig. 5.** Monthly zonal mean latitude-pressure cross-sections of $CH_4$ from CMAM (January 2004–December 2007) and ACE-FTS (February 2004–August 2008).

Figure 6 shows that the ratios ACE-FTS/CMAM generally are within 0.85–1.15 below 1 hPa, except at high latitudes where such agreement is only present up to 20 hPa in the Southern Hemisphere and up to 10 hPa in the Northern Hemisphere. Previous comparisons oft CMAM $CH_4$ with HALOE observations (Russell et al., 1993) also showed a good agreement below 1 hPa (Zhang, 2002; Eyring et al., 2006). Above this level, although the absolute difference between the simulated and observed VMR profiles is generally less than 0.2 ppmv, the ratios ACE-FTS/CMAM are significantly greater than unity. The maxima of the ratios range from 2–7, revealing a low bias in the CMAM simulation.

This low bias suggests that the vertical transport from the stratosphere to the mesosphere in the model is slower than in the real atmosphere. This is confirmed by the similarities between $CH_4$ and $N_2O$ biases in CMAM. Figure 6 shows the ratios ACE-FTS $N_2O$ observations to the CMAM $N_2O$ simulation at the ACE-FTS latitudes. Although the ratios for $N_2O$ are in general significantly larger than the ratios for $CH_4$, their departures from the value 1.0 occur at similar altitudes. Since the chemical destruction processes of $CH_4$ and $N_2O$ are different, this pattern strongly suggests that the negative biases are due to insufficient vertical transport in the upper stratosphere.
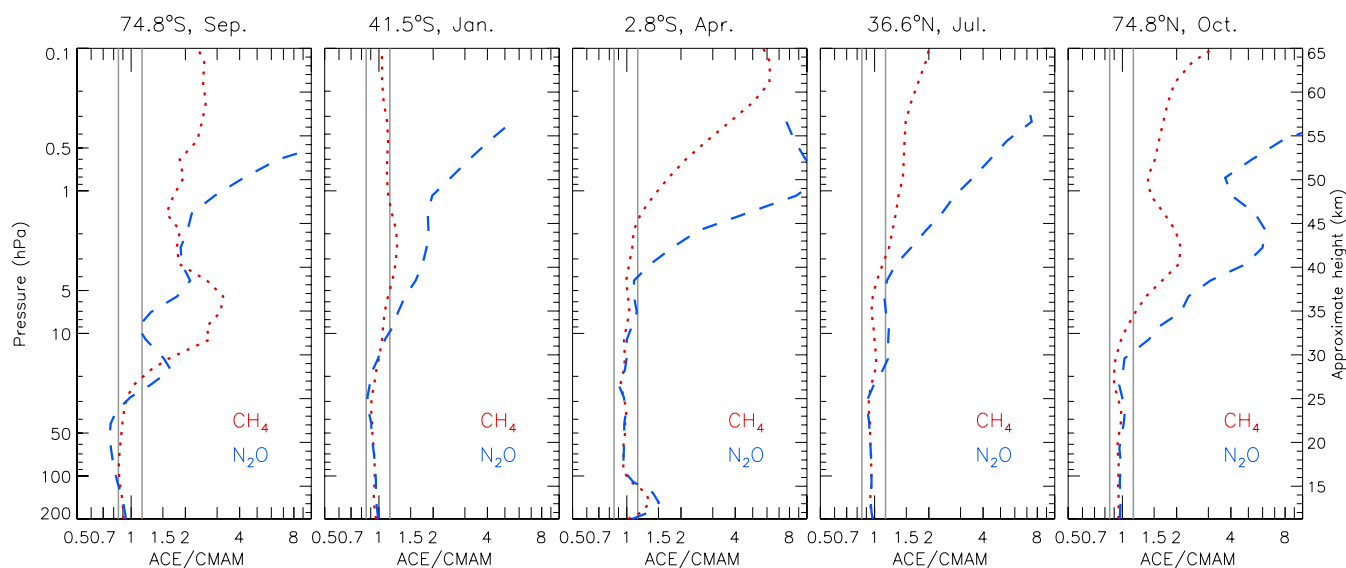
**Fig. 6.** Ratios of monthly mean for CH$_4$ (red dotted line) and N$_2$O (blue dashed line): ACE-FTS/(CMAM at the ACE-FTS latitudes). The ratios for N$_2$O are also shown in Fig. 4. The grey vertical straight lines indicate ratios 0.85 and 1.15. The N$_2$O and CH$_4$ VMRs are shown in Figs. 3 and 5, respectively.

The difference between the ratios for N$_2$O and CH$_4$ above ~10 hPa can perhaps be attributed to the treatment of vertical diffusion (K$_Z$) in the standard CMAM model. In the appendix, for a species whose profile is determined by chemical loss and transport, we show that its scale height is determined by a ratio connecting the chemical lifetime and the vertical diffusion. The scale height for a shorter-lived species is smaller than a relatively longer-lived species, and thus the mixing ratios of a short-lived species decrease more quickly than the relatively longer-lived species. In other words, if the diffusion is smaller in a model than in the atmosphere, the model results would have a larger negative bias for a relatively shorter-lived species than a relatively longer-lived species which is the case for N$_2$O versus CH$_4$. We note that in the CMAM version used in this study, the only vertical diffusion in the stratosphere and lower mesosphere is due to wind shear and due to a background eddy diffusion, but not due to the eddy diffusion generated by GWD. The local chemical lifetimes of N$_2$O and CH$_4$ are about a few weeks and a few months, respectively, in the upper stratosphere. Therefore, the simulated N$_2$O has a relatively larger negative bias than the simulated CH$_4$. An ongoing study shows that the behavior of N$_2$O and CH$_4$ can be improved by introducing the diffusion associated with the GWD in the stratosphere and lower mesosphere. As mentioned in Sect. 4, however, the advection instead of diffusion induced by GWD might be the primary factor for their negative biases.

# 6 Polar descent

Measurements of long lived species such as CO, CH$_4$, N$_2$O and H$_2$O indicate that polar mesospheric air can be transported downward into the stratosphere with a limited degree of dilution (e.g., Schoeberl et al., 1995; Manney et al., 1995, 2008a; Allen et al., 2000; Juckes, 2007) and this is also seen in transport calculations (e.g., Manney et al., 1994; Plumb et al., 2002). This phenomenon is related to the rapid and deep descent inside the polar vortex from late fall to early spring. Enhanced descent has also been observed recently in the upper stratosphere in the Arctic in early year 2004 and 2006 in the wake of prolonged major sudden stratospheric warmings (SSWs) (Manney et al., 2005, 2008b; Siskind et al., 2007). This enhanced descent creates a window for relatively confined transport of nitrogen oxides (NO$_x$) from the mesopause region in the polar night (e.g., Rinsland et al., 2005; Hauchecorne et al., 2007; Semeniuk et al., 2008).

In this section, we compare time-altitude slices of the polar descent in stratosphere and mesosphere from CMAM with recent CO measurements from MLS and ACE-FTS. At the same time, a full picture of observed annual evolution of CO in the polar stratosphere and mesosphere is provided. Measurements in the Arctic during periods July 2004–June 2005, and July 2005–June 2006 and averaged observations in the Antarctic during the period January 2005–December 2007 are used.

Panel (a) in Figs. 7 and 8 shows the MLS CO measurements near the North Pole (70° N–82° N) during periods of July 2004–June 2005 and July 2005–June 2006, respectively. Because the model results are from a climatological
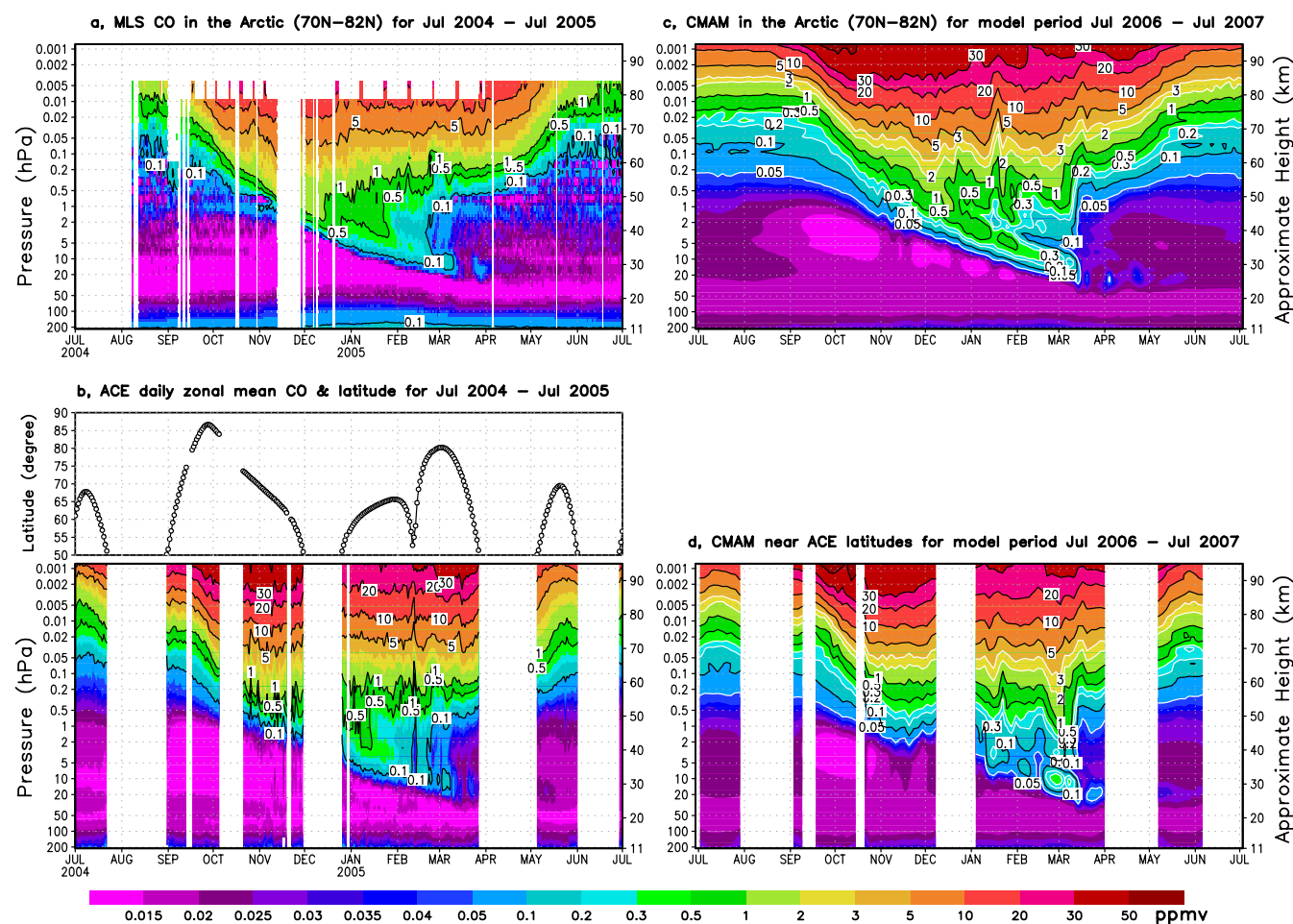
**Fig. 7.** Evolution of CO zonal averages from MLS (panel **a**) and ACE-FTS (panel **b**) measurements for the period July 2004–June 2005. Because exact reproduction of the observations in the same calendar year is not expected in a climatological simulation, CMAM results and CMAM results near the ACE-FTS latitudes in the Arctic for the model period July 2006–June 2007 when minor SSWs occurred in the model are shown in panel (**c**) and panel (**d**), respectively. The averaged latitudes of ACE-FTS are also shown in panel (b).

simulation, exact reproduction of the observations in each calendar year is not expected. So we choose the CMAM simulation in two model periods of July 2006–June 2007 and July 2004–June 2005 when minor and strong Arctic SSWs occur, respectively, as seen in the CO evolution (see panel c in Figs. 7 and 8), temperature and wind (now shown). In addition, the daily zonal mean of ACE-FTS CO observations north of 50° N for the periods of July 2004–June 2005 and July 2005–June 2006 are shown in panel (b) in Figs. 7 and 8, respectively. The CMAM zonal means near the ACE-FTS latitudes for the model periods of July 2006–June 2007 and July 2004–June 2005 are shown in panel (d) in Figs. 7 and 8, respectively.

The winter of 2004/2005 was identified as one of the coldest winters ever observed in the Arctic stratosphere and there was a strong stratospheric polar vortex before its early breakup in March 2005 (Manney et al., 2006, 2008a). As a result, significantly increased CO mixing ratios can be

seen in the stratosphere during the winter season (November 2004–March 2005) (see Fig. 7 panels a and b). Air containing 0.1 ppmv CO, located in the lower mesosphere at around 0.1 hPa (~60 km) in late September 2004, descended to 20 hPa (~28 km) in some locations by mid-March 2005, reflecting rapid downward transport in the polar region: of course there is no CO production and its loss is extremely slow during the polar night. In mid-March 2005, the stratospheric vortex broke up and the high CO mixing ratio air was quickly diluted with low CO mixing ratio air from midlatitudes. The Arctic stratosphere CO evolution during the winters of 2004/2005 and 2005/2006 is also shown by Manney et al. (2007, 2008a). In the winter mesosphere, where the lifetime of CO is very long, the CO concentration stabilized above around 0.1 hPa (~60 km) after the rapid increase in September–October, and the CO enriched air was not diluted until April/May 2005. The rapid increase in fall and decrease in spring are related to the onset of descent and
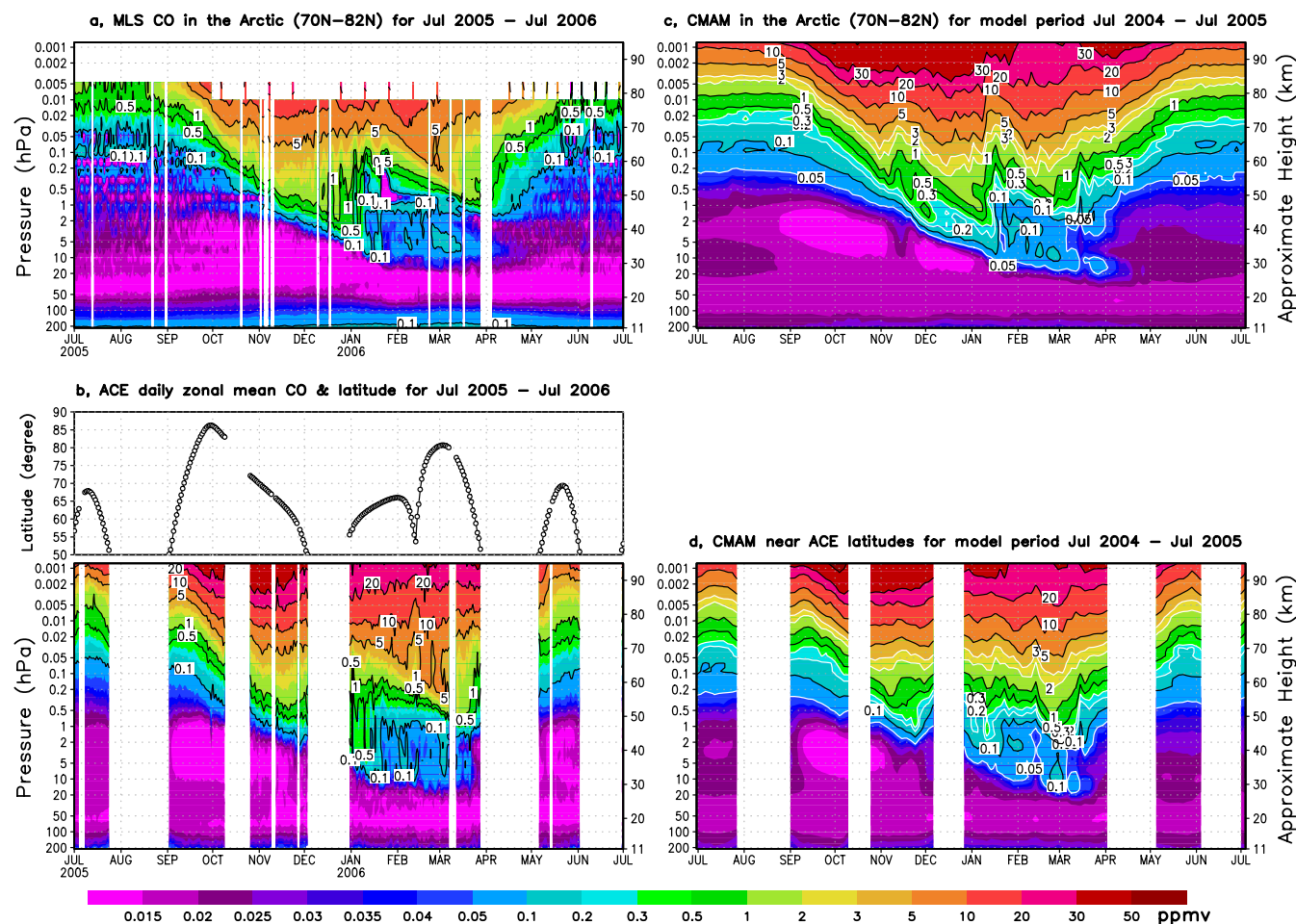
**Fig. 8.** Evolution of CO zonal averages. They are the same as Fig. 7, but the observation period of MLS and ACE-FTS is July 2005–June 2006 and the model period is July 2004–June 2005 when strong SSWs occurred.

ascent, respectively, resulting from the mesospheric pole-to-pole meridional circulation (Plumb, 2002; Shepherd, 2007). The flatness of the CO isopleths in the winter mesosphere indicates that an equilibrium between vertical transport and horizontal mixing is established quickly and maintained.

The CMAM simulation shown in panel (c) in Fig. 7 has a very similar morphology to the MLS measurements. There is similar descent of CO rich air from mesosphere into the lower stratosphere from fall to spring and CO decrease in later spring. However, there is a significant reduction of CO in the middle and upper stratosphere after mid-January, which is due to a SSW and the associated mixing with mid-latitude low CO mixing ratio air. This is more clearly seen in measurements and simulations with strong SSWs as discussed below. The CMAM results also follow ACE-FTS measurements (see panels b and d) very well over the Arctic regions throughout the year. Around 1 March, however, CMAM is larger than ACE-FTS above 10 hPa. In fact, CMAM is also larger than the MLS above 10 hPa near the

North Pole around 1 March. This difference can be attributed to the strong vortex in the selected model period and the early breakup of the Arctic stratospheric vortex in March 2005 although it was very strong in January and February 2005 (Manney et al., 2007, 2008a).

Panel (a) in Fig. 8 shows the Arctic CO evolution observed by MLS in 2005/2006 winter when a strong and long-lasting SSW occurred in early January 2006 (Manney et al., 2008b). As a result, the high CO air was rapidly diluted in mid-January below 0.1 hPa (~60 km). However, the mesospheric air above was not disturbed until late January 2006. Previous studies have shown that the stratopause broke down in late January, then reformed at about 0.01 hPa (~75 km) and a cold upper stratospheric vortex formed below it (Siskind et al., 2007; Manney et al., 2008b). After that, the air isolated in this recovered vortex started to descend above 0.5 hPa, and the downward tongue, which is a distinct feature from the 2004/2005 winter, is seen in the upper stratosphere and lower mesosphere (above 2 hPa) in the spring. The CO

concentration is even larger than that before the SSW. This CO downward tongue is also observed by ACE-FTS (see panel b, also shown by Randall et al., 2006).

Panel (c) in Fig. 8 shows CMAM Arctic simulations with a major SSW in January and two minor SSWs in November and March. The major SSW that happened to develop in one of the four model years is not as strong as seen in the observations so that CO is not diluted to pre-vortex background values (compare with panels a and b). Although the mesospheric CO is immediately disturbed by the SSW in the simulation and the CO mixing ratio after the SSW is not larger than that before the SSW as the case in the observations, the descent of air with large CO from the mesosphere into the stratosphere after the SSW agrees with the observations of downward transport following a strong SSW in midwinter. Moreover, the evolution of the model temperature (not shown) does exhibit features similar to previous observations (Manney et al., 2008b): The temperature decreases by over 20 K in the upper stratosphere and lower mesosphere after the SSW. We also note that there is a CO disturbance in the upper stratosphere in November and March in the model results. CMAM zonal means near the ACE-FTS latitudes are shown in panel (d). Although the CMAM model results at the northern high latitudes show the CO enhancement after the major SSW (panel c), CMAM results sampled near the ACE-FTS locations do not display this feature, which suggests that the restored upper-level vortex is too small and short-lived. However, we note that the difference does not necessarily point to a deficiency in the model since the simulated SSW is modeled in a climate model and is not expected to match exactly the strong SSW during the 2006 winter. Obviously, further investigation of the characteristics of the model's SSW behavior is needed.

Figure 9 shows the multi-year averaged CO in the Antarctic from MLS (panel a), ACE-FTS (panel c) and CMAM (panels b and d). They all demonstrate very similar annual CO evolutions throughout the domain. However, CMAM mixing ratios are larger than MLS values in the mesosphere from April to October. The modeled air with 1 ppmv CO at high southern latitudes is found at lower altitudes (about 2 hPa) than in the MLS measurements (about 0.5 hPa) in July. Furthermore, the CO tongue, which reflects the residual stratospheric vortex at high latitudes in late spring, did not vanish until late November in the model results (panel b), while it disappeared at the beginning of November in the MLS measurements. The CO distributions of ACE-FTS and CMAM are generally very similar throughout the year. The CO tongue shown by MLS and CMAM in panels (a) and (c) does not extend into the lower stratosphere in ACE-FTS and CMAM-sampled-ACE latitudes because of the absence of ACE-FTS observations at high latitudes in October. However, CMAM does show a maximum at 20 hPa–10 hPa in November while it is not evident in ACE-FTS measurements. All these differences suggest that CMAM has a later breakup of the Antarctic polar vortex than the real atmosphere,

consistent with previous studies (Shepherd, 2000; Eyring et al., 2006).

An inter-hemispheric comparison shows a similar mesospheric CO morphology above about 0.1 hPa (∼60 km) in the Antarctic to that in the Arctic in the absence of a major SSW. However, there is a prolonged stratospheric CO enhancement in the Antarctic in spring, because the stratospheric vortex in the Antarctic is generally stronger and longer lasting than in the Arctic.

# 7 Comparisons of tropical oscillations

In the tropics, convection and land-sea surface contrasts drive strong wave activity that propagates into the middle atmosphere (e.g., Baldwin et al., 2001, and references therein). This wave activity can leave its signature on the distribution of minor species. For example, the water vapour and CO "tape recorders" (e.g., Mote et al., 1996; Randel et al., 2001; Schoeberl et al., 2006) in the upper troposphere and lower stratosphere (UT/LS), the quasi-biennial oscillation (QBO) and the semi-annual oscillation (SAO) in ozone and water vapour in the stratosphere and mesosphere (e.g., Ray et al., 1994; Garcia et al., 1997; Dunkerton, 2001; Tian et al., 2006; Huang et al., 2008). Schoeberl et al. (2006) suggested that the CO tape recorder signal (or annual oscillation) in the lower stratosphere is partly due to seasonal changes of surface sources such as biomass burning. Thus the behavior of this signal is superimposed on the dynamical signature. Other studies have shown that the signal is driven by the tropical upwelling due to annual temperature oscillation (Randel et al., 2007) and by the Brewer-Dobson circulation (Schoeberl et al., 2008) in the lower stratosphere. The SAO and QBO in the chemical tracers are also determined by the wind and temperature oscillations associated with the middle atmospheric circulation (e.g., Gray and Pyle, 1986; Ray et al., 1994; Baldwin et al., 2001).

In this section, we qualitatively compare the signals in the CMAM simulation with those in the satellite observations. We note that ACE-FTS observations are not used in this section. Because the prime objectives for SCISAT-1 were focused on polar regions the orbit design yielded limited coverage of the tropics, although careful use of them has produced valuable information on seasonal convective outflow at the tropical tropopause (Folkins et al., 2006) and the tropical tape recorder of HCN (Pumphrey et al., 2008).

First, the CMAM results show a morphology similar to the observed CO annual oscillation in the lower stratosphere. Figure 10 shows the multi-year averages of CO anomalies, which are the observed or simulated daily zonal means minus annual zonal means, in the tropics. In panel (a), MLS CO observations demonstrate a seasonal variation below 50 hPa (20 km), which was identified as a tape recorder-like (annual oscillation) signal linked to the seasonal change of biomass burning by Schoeberl et al. (2006). In panel (b), the seasonal
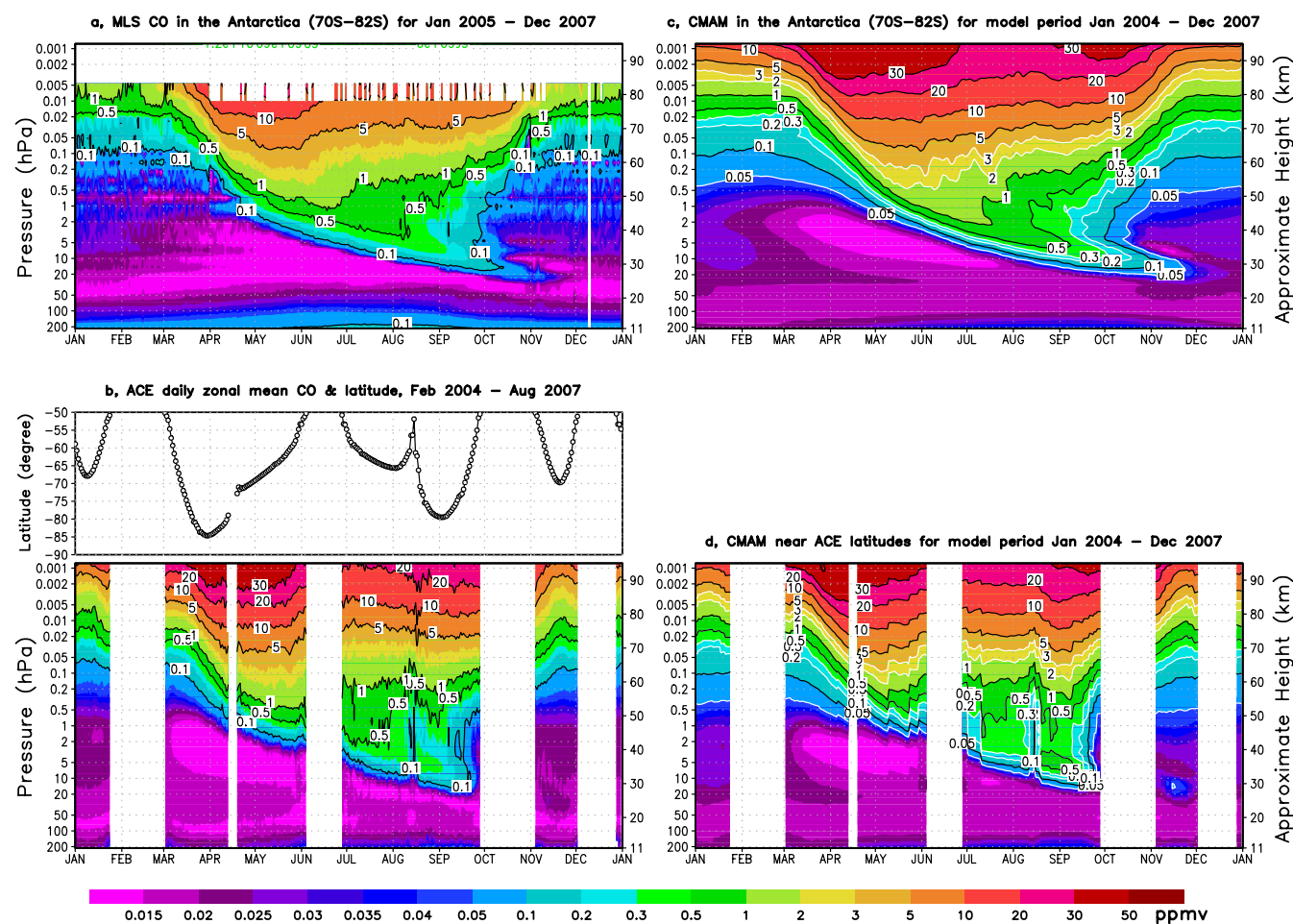
**Fig. 9.** Evolution of CO multi-year zonal averages from MLS (panel **a**) and ACE-FTS (panel **b**) measurements, CMAM results (panel **c**), and CMAM results at the ACE-FTS latitudes in the Antarctic (panel **d**).

variation of CMAM CO is evident between 100–50 hPa (16–20 km). The +1 ppbv positive anomaly and −1 ppbv negative anomaly start from December and July, respectively. The maximum and the minimum values of the anomalies are about +3 ppbv and −3 ppbv, respectively. As noted above there are no biomass burning sources in the simulation, therefore the oscillation reveals a purely dynamical signal. Its amplitude is thus expected to be smaller than in the observations. As a result, the upper tropospheric (below 150 hPa) CO enhancement is not seen in the model. Aside from these differences, the oscillation in the model shows a similar temporal evolution of the upward motion in the lower stratosphere. Since the upper tropospheric variation is not significant, the model variation suggests that diabatic upwelling and the Brewer-Dobson circulation, which are also indentified as factors for the annual oscillation (Schoeberl et al., 2008), are reasonably well characterized in the model.

Figure 10 shows another feature common in the observations and model: the SAO of tracer concentrations at the mesopause and stratopause. Two large CO positive anoma-

lies occur above ∼0.01 hPa (∼85 km) in April–May and October–November in both CMAM and MLS, suggesting presence of a significant SAO signal at the mesopause. The one occurring in the first half of the calendar year stays at the mesopause and decreases quickly to a negative anomaly in June. However, the one in the second half of the calendar year descends during the subsequent months and reaches the stratopause (about 1 hPa) in February–March when it merges with one of the positive anomalies at the stratopause. At the stratopause, CMAM exhibits another positive anomaly in September–October. Descent of the positive and negative anomalies originating at the stratopause in the first half of the calendar year (and subsequent months too) can be seen above about 10 hPa (35 km). However, the anomalies originating at the stratopause in the second half of the year stay above ∼3 hPa (40 km). The MLS CO measurements exhibit similar semi-annual oscillations in the middle and upper stratosphere (panels a). There is also a clear downward propagation of the first pair of anomalies while it is not evident for the second pair.
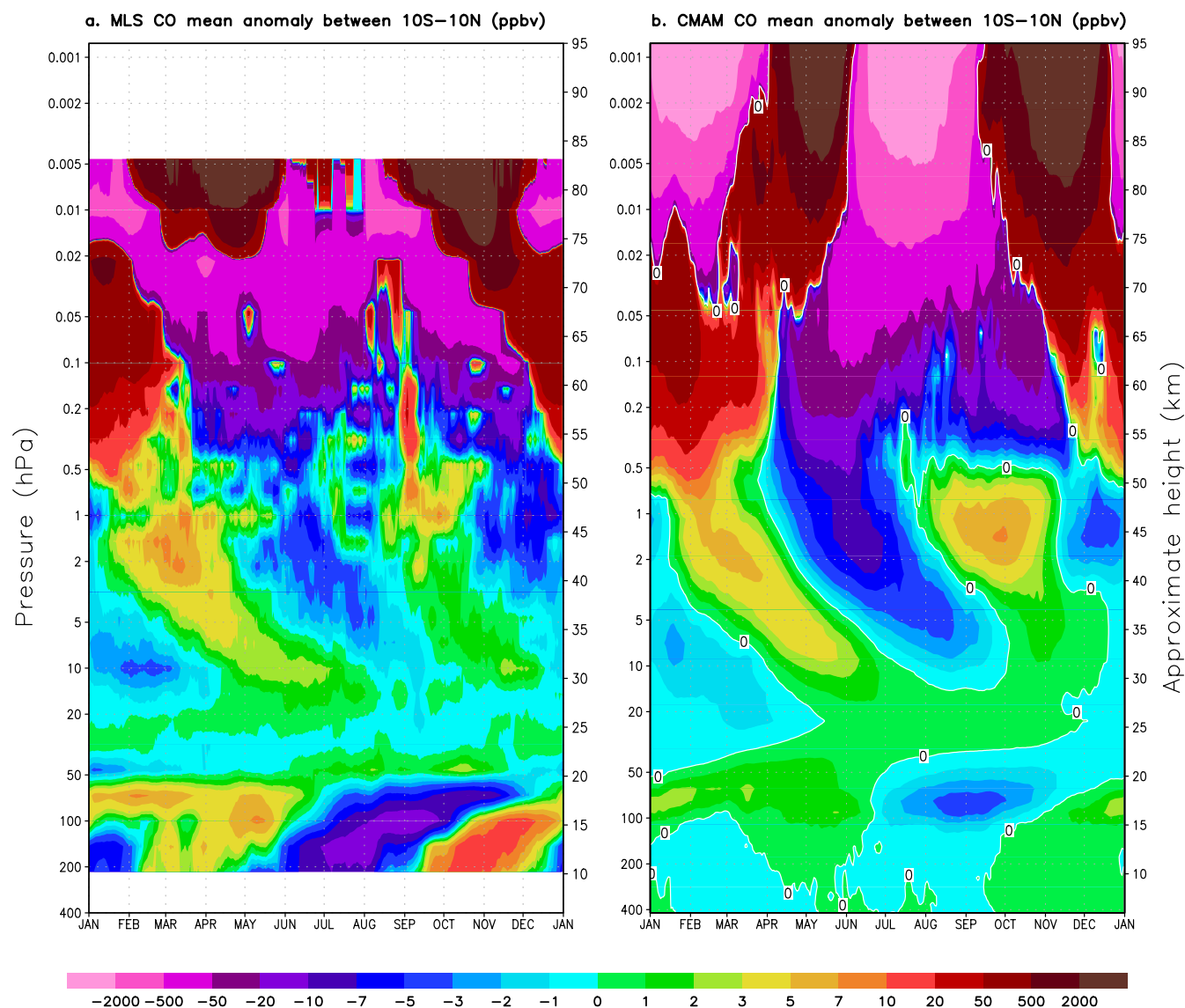
**Fig. 10.** Multi-year average of the tropical CO anomalies of MLS (panel **a**, August 2004–April 2008) and CMAM (panel **b**, January 2004–December 2007). The anomalies are the daily zonal means minus annual zonal means. The MLS panel is smoothed with 10-day running average.

The SAO in the CO field is in phase with the oscillations of model temperature (not shown) and observed temperature at the mesopause, consistent with expectations from previous studies (Garcia et al., 1997): the positive anomaly of CO is associated with the warm anomaly in the temperature field. The positive anomaly is also associated with the observed westerly wind shear (Hirota, 1978; Garcia et al., 1997). When considering that CO increases with height in the mesosphere, we may conclude that the positive anomaly of CO is driven by the descent associated with a secondary meridional circulation during the westerly phase of the oscillation (Andrews et al., 1987). In addition, the SAO in MLS and CMAM CO fields is in phase with the SAO in the SABER (Sound-

ing of the Atmosphere using Broadband Emission Radiometry) $O_3$ field above 0.01 hPa ($\sim$80 km) (Huang et al., 2008). This is not surprising since $O_3$ also increases with height due to the local chemical production in the tropical mesosphere. However, the CO field shows a strong annual oscillation between 0.5–0.05 hPa (50–70 km), while the SABER $O_3$ field shows the SAO. The reason for this difference is not clear at the moment.

The SMR and MLS $N_2O$ measurements also show an SAO signature at the stratopause (panels a and b, Fig. 11). We find that the CMAM $N_2O$ oscillations have in general good agreement with the SMR and MLS measurements but have a smaller amplitude except for the spatially larger anomaly at
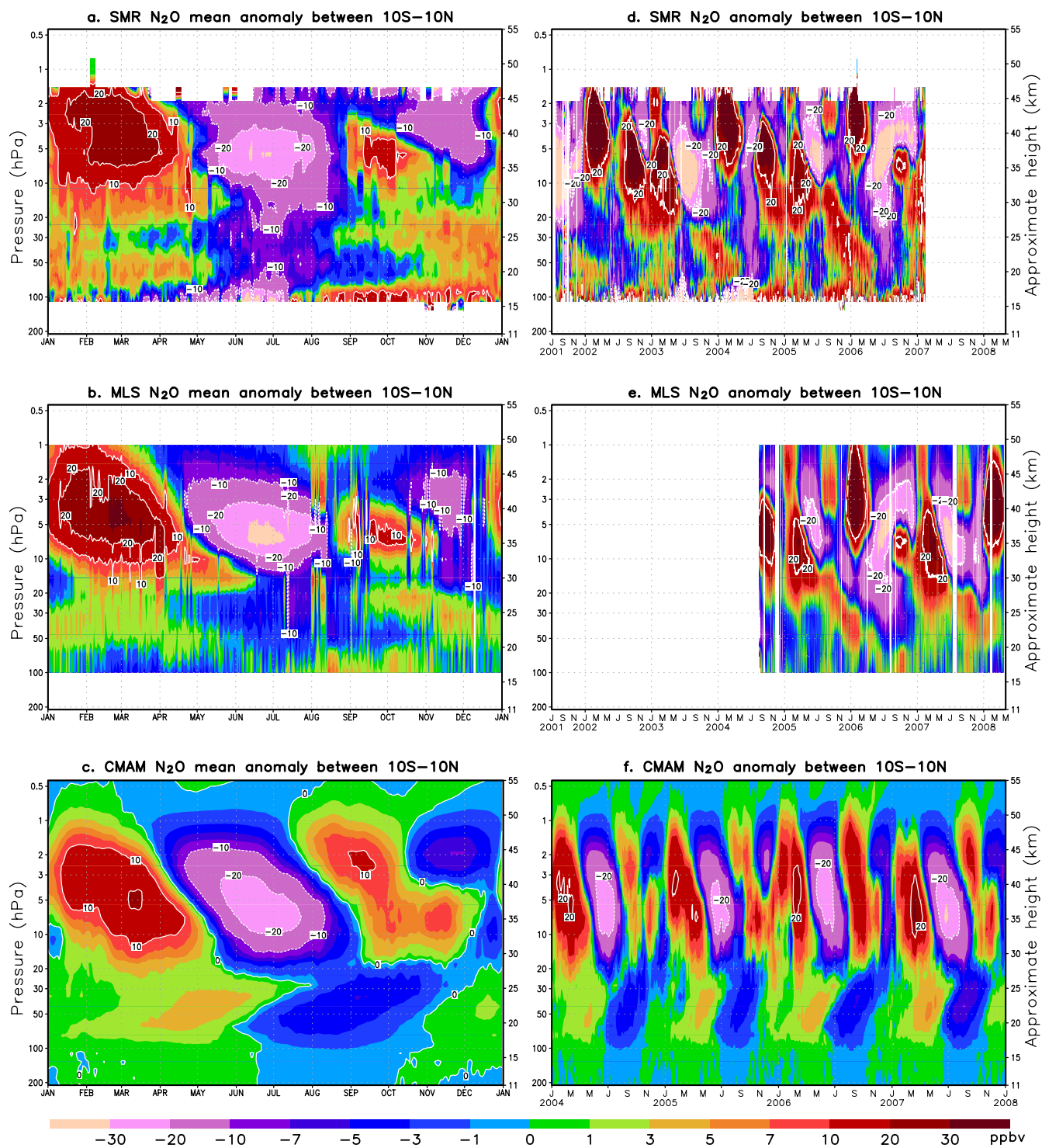
**Fig. 11.** Multi-year average of the tropical N$_2$O anomalies (see Fig. 10) for SMR (panel **a**, July 2001–February 2007), MLS (panel **b**, August 2004–April 2008) and CMAM (panel **c**, January 2004–December 2007). Panels **(d)**, **(e)** and **(f)** show the anomalies (daily zonal means minus multi-year zonal means) for SMR, MLS and CMAM N$_2$O.

2 hPa in September. Both measurements and model results show that the first cycle in the calendar year is stronger than the second. The SAO is also evident in the CMAM $CH_4$ field (not shown), and the maximum amplitude of the $CH_4$ anomalies exceeds 100 ppbv at the stratopause. In addition, the SAOs in CMAM stratospheric $N_2O$ and $CH_4$ fields are locked in phase, which is not surprising since $N_2O$ and $CH_4$ are similar long-lived tracers in the stratosphere and both are emitted from the Earth's surface.

The similarity of the SAO signal in the both observed and simulated $N_2O$ fields suggests that the model is capturing important dynamical features. The temperature SAO at the stratopause in CMAM (not shown) is also in good agreement with that in the SABER observations reported by Huang et al. (2008). Comparisons of the zonal wind SAO at the stratopause in CMAM (Medvedev and Klaassen, 2001) and observations (Hirota, 1978; Garcia et al., 1997) indicate that the positive anomalies in these tracers are associated with easterly wind shear and negative temperature anomalies while the negative anomalies in the tracers are associated with westerly wind shear and positive temperature anomalies. This is also consistent with the understanding of the SAO in long-lived tracers (e.g., Gray and Pyle, 1986; Ray et al., 1994).

The anomalies in the CO field are also in phase with the anomalies of $N_2O$ and $CH_4$ at the stratopause. When considering that CO is produced from $CH_4$ in the stratosphere, we can attribute the SAO of CO to the oscillations of $CH_4$.

In addition, the SMR $N_2O$ field shows a quasi-biennial oscillation in the upper stratosphere. The SMR $N_2O$ anomalies, which are daily zonal mean minus a multi-year (July 2001–February 2007) zonal mean, are shown in Fig. 11, panel (d). It can be seen that the large positive anomalies propagate downward in the upper stratosphere and the temporal interval between the propagation is about two years. Comparing with the QBO of the zonal wind given in Schoeberl et al. (2008) in the middle stratosphere, it is found that the QBO is in its westerly phase (the wind is westerly at 40 hPa) during the years 2002, 2004 and 2006 when the first positive $N_2O$ anomaly in the calendar year occurs at relative higher altitudes, while the QBO is in its easterly phase during the years 2003 and 2005 when the first positive anomaly in the calendar years occurs at relative lower altitudes. The MLS $N_2O$ field also shows a quasi-biennial oscillation in the upper stratosphere. In addition, the variation is very similar to that in the SMR $N_2O$ field during the overlap period August 2004–January 2007. Details about the phase and amplitude of the MLS $N_2O$ SAO and QBO can be found in Schoeberl et al. (2008). The CMAM $N_2O$ anomalies over a 4-year mean are shown in Fig. 11, panel (f). Since the version of the model used in this study does not have the dynamical QBO included, it is not surprising to see that the chemical species in the model results fail to show the quasi-biennial oscillation in the upper stratosphere.

# 8 Summary

In order to further evaluate the chemistry climate model CMAM, model results for CO, $N_2O$ and $CH_4$ have been compared with the recent measurements from the satellite instruments SMR, ACE-FTS, and Aura/MLS. The comparison shows a good agreement between the model results and observations. However, CMAM has a negative bias in $N_2O$ and $CH_4$ in the upper stratosphere, which might be due to the slow advection related to the GWD scheme in the model.

CMAM reproduces the main characteristics of the CO distribution and temporal evolution very well. The differences between the model and the ACE-FTS measurements are generally less than 30% in the middle atmosphere and the agreement between the model results and the SMR and MLS measurements are slightly worse. However, the differences between the model results and measurements are comparable with the difference between the instruments (see also Pumphrey et al., 2007). We note CMAM has a positive bias in the Antarctic middle stratosphere in spring due to the stronger Antarctic vortex in the model than in the real atmosphere. In the lower stratosphere and upper troposphere, CMAM CO values are smaller than the measurements because of the absence of a realistic implementation of important tropospheric processes in the model. However, differences between measurements are also large, suggesting that improvements in the measurements and/or retrieved values in this region are needed.

CMAM also reproduces the seasonal CO variation at high latitudes very well. All the measurements and the model results show the strong meridional increase towards the winter polar regions, which is due to the meridional transport in the mesosphere and descent into the stratospheric polar vortex. The complete annual evolution of CO in the Arctic and Antarctic is also presented in this study. Both the observations and simulation show that mesospheric air can descend into stratosphere as low as 20 hPa in both the Arctic and Antarctic. However, in the Antarctic the large CO concentrations in the lower stratosphere in November indicate that the CMAM polar vortex is too persistent. In addition, the ACE and MLS CO measurements demonstrate strong descent in the recovery phase of the upper stratospheric Arctic polar vortex following the SSW in the 2006 winter. CMAM also shows this rapid descent in the upper stratospheric polar vortex in the wake of a SSW. However, CMAM sampled at the ACE-FTS latitudes does not show this feature. We note that the comparison here is between a climatological simulation and observations in a particular year and thus the difference does not necessary mean there is a deficiency in the model although further investigation of the model's behavior during and after SSWs is needed.

CMAM simulates the lower and middle stratospheric $N_2O$ and $CH_4$ very well. The CMAM results are generally within 15% of the $N_2O$ and $CH_4$ measurements. In general, the "mixing barriers" which are evident in the CMAM

monthly mean cross-sections are quite realistic. The model-measurement comparison has, however, highlighted the need for improvement of the vertical sub-grid scale diffusion in CMAM. In the upper stratosphere, CMAM $N_2O$ and $CH_4$ are significantly smaller than these measurements. A test (not shown) suggests that these negative biases can be reduced by introducing a vertical diffusion coefficient related to gravity wave drag. However, our other study shows that GWD schemes have strong impact on the vertical advection in the upper stratosphere. Further studies on the impact of the GWD schemes on the distribution of the species are needed.

CMAM captures the tropical annual oscillation in the upper troposphere and lower stratosphere. The absence of biomass and fossil fuel burning emissions in the model simulation allows for a clear signature of the annual variation of tropical upwelling in the CO. The CO transport indicates that CMAM has a reasonable upward motion in the tropical lower stratosphere. Although the QBO shown by the SMR and MLS $N_2O$ observations in the upper stratosphere is not reproduced by the model, the SAOs in CMAM generally show good agreement with the observations at the stratopause and mesopause.

## Appendix A

### Scale height for species

When considering a simple one-dimension model, the vertical flux, $\varphi_i$, of a species "$i$" of volume mixing ratio $f_i$ is given by

$$\varphi_i = -K_Z M \frac{df_i}{dz} \tag{A1}$$

where $K_Z$ is the vertical eddy diffusion coefficient and is, for simplicity, assumed to be a constant although it varies with atmospheric conditions and chemical species (Andrews et al., 1987). $M$ is the total air number density. If the species has no local chemical source but only a loss process of frequency $L_i$, the continuity equation can be written in steady state

$$\frac{d\varphi_i}{dz} = -L_i f_i M \tag{A2}$$

Combining these into a single equation and assuming that the atmosphere is isothermal with scale height, $H_{av}$, we obtain

$$\frac{d^2 f_i}{dz^2} - \frac{1}{H_{av}} \frac{df_i}{dz} - \frac{L_i}{K_Z} f_i = 0 \tag{A3}$$

If we assume that $f_i = f_{i0} \exp(-\alpha_i z)$, then substituting it into Eq. (A3), we find that $\alpha_i$ satisfies

$$\alpha_i^2 + \frac{1}{H_{av}} \alpha_i - \frac{L_i}{K_Z} = 0 \tag{A4}$$

or $\alpha_i$ is given by

$$\alpha_i = -\frac{1}{2H_{av}} \pm \sqrt{\frac{1}{(2H_{av})^2} + \frac{L_i}{K_Z}}$$

$$= -\frac{1}{2H_{av}} \pm \frac{1}{2H_{av}} \sqrt{1 + \frac{4H_{av}^2 L_i}{K_Z}} \tag{A5}$$

The role of the chemical lifetime is made more explicit if we look at limiting cases when the second term under the square root is both $\gg 1$ and $\ll 1$ which will occur for short-lived and long-lived species (short and long-lived in the context of a given $K_Z$), respectively. For the first case ("short-lived" species) which for $K_Z \sim 1\,m^2\,s^{-1}$, $H_{av} \sim 7\,km$ then $L_i \gg 10^{-7}\,s^{-1}$ or a local chemical time constant $\ll 3$ months. In this case, neglecting the first term on the right hand side we obtain $\alpha_i = \sqrt{L_i/K_Z}\,m^{-1}$ or the scale height of the minor species mixing ratio,

$$H_i = 1/\alpha_i = \sqrt{K_Z/L_i}\,m \tag{A6}$$

For long-lived species expanding the term under the square root sign and choosing the positive root we obtain

$$H_i = 1/\alpha_i \approx +\frac{K_Z}{H_{av} L_i}\,m \tag{A7}$$

In each case the scale height is affected by the chemical lifetime, $\tau_{chem} = 1/L_i$.

## References

Allen, D. R., Stanford, J. L., López-Valverde, M. A., Nakamura, N., Lary, D. J., Douglass, A. R., Cerniglia, M. C., Remedios, J. J., and Taylor, F. W.: Observations of middle atmosphere CO from the UARS ISAMS during the early northern winter 1991/1992, J. Atmos. Sci., 56, 563–583, 1999.

Allen, D. R., Stanford, J. L., Nakamura, N., López-Valverde, M. A., López-Puertas, M., Taylor, F. W., and Remedios, J. J.: Antarctic polar descent and planetary wave activity observed in ISAMS CO from April to July 1992, Geophys. Res. Lett., 27(5), 665–668, 2000.

Andrews, D. G., Holton, J. R., and Leovy, C. B.: Middle Atmospheric Dynamics, Academic Press, 1–489, 1987.

Baldwin, M. P., Gray, L. J., Dunkerton, T. J., Hamilton, K., Haynes, P. H., Randel, W. J., Holton, J. R., Alexander, M. J., Hirota, I., Horinouchi, T., Jones, D. B. A., Kinnersley, J. S., Marquardt, C., Sato, K., and Takahashi, M.: The Quasi-Biennial Oscillation, Rev. Geophys., 39(2), 179–229, 2001.

Barret, B., Ricaud, P., Santee, M. L., Attié, J.-L., Urban, J., Le Flochmoën, E., Berthet, G., Murtagh, D., Eriksson, P., Jones, A., De La Noë, J., Dupuy, E., Froidevaux, L., Livesey, N. J., Waters, J. W., and Filipiak, M. J.: Intercomparisons of trace gases profiles from the Odin/SMR and Aura/MLS limb sounders, J. Geophys. Res., 111, D21302, doi:10.1029/2006JD007305, 2006.

Beagley, S. R., de Grandpré, J., Koshyk, J. N., McFarlane, N. A., and Shepherd, T. G.: Radiative-dynamical climatology of the first-generation Canadian Middle Atmosphere Model, Atmos.-Ocean, 35(3), 293–331, 1997.

Bernath, P. F., McElroy, C. T., Abrahams, M. C., et al.: Atmospheric Chemistry Experiment (ACE): Mission overview, Geophys. Res. Lett., 32, L15S01, doi:10.1029/2005GL022386, 2005.

Boone, C. D., Nassar, R., Walker, K. A., Rochon, Y., McLeod, S. D., Rinsland, C. P., and Bernath, P. F.: Retrievals for the atmospheric chemistry experiment Fourier-transform spectrometer, Appl. Optics, 44(33), 7218–7231, 2005.

Brasseur, G. P. and Solomon, S.: Aeronomy of the middle atmosphere, 3rd ed., Springer, Dordrecht, The Netherlands, pp. 1–646, 2005.

Clerbaux C., Coheur, P.-F., Hurtmans, Barret, B., Carleer, M., Colin, R., Semeniuk, K., McConnell, J. C., Boone, C., and Bernath P. F.: Carbon monoxide distribution from the ACE-FTS solar occultation measurements, Geophys. Res. Lett., 32, L16S01, doi:10.1029/2005GL022394, 2005.

Clerbaux, C., George, M., Turquety, S., Walker, K. A., et al.: CO measurements from the ACE-FTS satellite instrument: data analysis and validation using ground-based, airborne and spaceborne observations, Atmos. Chem. Phys., 8, 2569–2594, 2008, http://www.atmos-chem-phys.net/8/2569/2008/.

de Grandpré, J., Beagley, S. R., Fomichev, V. I., Griffioen, E., McConnell, J. C., Medvedev, A. S., and Shepherd, T. G.: Ozone climatology using interactive chemistry: Results from the Canadian Middle Atmosphere Model, J. Geophys. Res., 105(D21), 26475–26492, doi:10.1029/2000JD900427, 2000.

De Mazière, M., Vigouroux, C., Bernath, P. F., et al.: Validation of ACE-FTS v2.2 methane profiles from the upper troposphere to the lower mesosphere, Atmos. Chem. Phys., 8, 2421–2435, 2008, http://www.atmos-chem-phys.net/8/2421/2008/.

Dunkerton, T. J.: Quasi-Biennial and Subbiennial Variations of Stratospheric Trace Constituents Derived from HALOE Observations, J. Atmos. Sci, 58(1), 7–25, 2001.

Dupuy, E., Urban, J., Ricaud, P., Le Flochmoën, É., Lautié, N., Murtagh, D., De La Noë, J., El Amraoui, L., Eriksson, P., Forkman, P., Frisk, U., Jégou, F., Jiménez, C., and Olberg, M.: Strato-mesospheric measurements of carbon monoxide with the Odin Sub-Millimetre Radiometer: Retrieval and first results, Geophys. Res. Lett., 31, L20101, doi:10.1029/2004GL020558, 2004.

Eyring, V., Butchart, N., Waugh, D. W., et al.: Assessment of temperature, trace species, and ozone in chemistry-climate model simulations of the recent past, J. Geophys. Res., 111, D22308, doi:10.1029/2006JD007327, 2006.

Eyring, V., Waugh, D. W., Bodeker, G. E., et al.: Multi-model projections of stratospheric ozone in the 21st century. J. Geophys. Res., 112, D16303, doi:10.1029/2006JD008332, 2007.

Folkins, I., Bernath, P., Boone, C., Lesins, G., Livesey, N., Thompson, A. M., Walker, K., and Witte, J. C.: Seasonal cycles of $O_3$, CO, and convective outflow at the tropical tropopause, Geophys. Res. Lett., 33, L16802, doi:10.1029/2006GL026602, 2006.

Fomichev, V. I., Fu, C., de Grandpré, J., Beagley, S. R., Ogibalov, V. P., and McConnell, J. C.: Model thermal response to minor radiative energy sources and sinks in the middle atmosphere, J. Geophys. Res., 109, D19107, doi:10.1029/2004JD004892, 2004.

Fomichev, V. I., Jonsson, A. I., de Grandpré, J., Beagley, S. R., McLandress, C., Semeniuk, K., and Shepherd, T. G.: Response of the Middle Atmosphere to $CO_2$ Doubling: Results from the Canadian Middle Atmosphere Model, J. Climate, 20(7), 1121–1144, 2007.

Froidevaux, L., Livesey, N. J., Read, W. G., et al.: Early validation analyses of atmospheric profiles from EOS MLS on the Aura satellite, IEEE Trans. Geosci. Remote Sensing, 44(5), 1106–1121, 2006.

Garcia, R. R., Dunkerton, T. J., Lieberman, R. S., and Vincent, R. A.: Climatology of the semiannual oscillation of the tropical middle atmosphere, J. Geophys. Res., 102(D22), 26019–26032, 1997.

Gray, L. J. and Pyle, J. A.: The semi-annual oscillation and equatorial tracer distributions, Q. J. Roy. Meteorol. Soc., 112, 387–407, 1986.

Hauchecorne, A., Bertaux, J.-L., Dalaudier, F., Russell III, J. M., Mlynczak, M. G., Kyrölä, E., and Fussen, D.: Large increase of $NO_2$ in the north polar mesosphere in January–February 2004: Evidence of a dynamical origin from GOMOS/ENVISAT and SABER/TIMED data, Geophys. Res. Lett., 34, L03810, doi:10.1029/2006GL027628, 2007.

Hirota, I.: Equatorial Waves in the Upper Stratosphere and Mesosphere in Relation to the Semiannual Oscillation of the Zonal Wind, J. Atmos. Sci., 35(4), 714–722, 1978.

Huang, F. T., Mayr, H. G., Reber, C. A., Russell III, J. M., Mlynczak, M. G., and Mengel, J. G.: Ozone quasi-biennial oscillations (QBO), semiannual oscillations (SAO), and correlations with temperature in the mesosphere, lower thermosphere, and stratosphere, based on measurements from SABER on TIMED and MLS on UARS, J. Geophys. Res., 113, A01316, doi:10.1029/2007JA012634, 2008.

Intergovernmental Panel on Climate Change (IPCC), Climate Change 2001: The scientific basis. Contribution of Working Group 1 to the Third Assessment Report, edited by: Houghton, J. T., Ding, Y., Griggs, D. J., Noguer, M., van der Linden, P. J., and Xiaosu, D., Cambridge Univ. Press, New York, 2001.

Jin, J. J., Semeniuk, K., Jonsson, A. I., Beagley, S. R., McConnell, J. C., Boone, C. D., Walker, K. A., Bernath, P. F., Rinsland, C. P., Dupuy, E., Ricaud, P., De la Noe, J., Urban, J., and Murtagh, D.: Co-located ACE-FTS and Odin/SMR stratospheric-mesospheric CO 2004 measurements and comparison with a GCM, Geophys. Res. Lett., 32, L15S03, doi:10.1029/2005GL022433, 2005.

Jonsson A. I., de Grandpré, J., Fomichev, V. I., McConnell, J. C., and Beagley, S. R.: Doubled $CO_2$-induced cooling in the middle atmosphere: Photochemical analysis of the ozone radiative feedback, J. Geophys. Res., 109, D24103, doi:10.1029/2004JD005093, 2004.

Juckes, M. N.: An annual cycle of long lived stratospheric gases from MIPAS, Atmos. Chem. Phys., 7, 1879–1897, 2007, http://www.atmos-chem-phys.net/7/1879/2007/.

Lambert, A., Read, W. G., Livesey, N. J., et al.: Validation of the Aura Microwave Limb Sounder middle atmosphere water vapor and nitrous oxide measurements, J. Geophys. Res., 112, D24S36, doi:10.1029/2007JD008724, 2007.

Livesey, N. J., Filipiak, M. J., Froidevaux, L., et al.: Validation of Aura Microwave Limb Sounder O3 and CO observations in the upper troposphere and lower stratosphere, J. Geophys. Res. 113, D15S02, doi:10.1029/2007JD008805, 2008.

Manney, G. L., Zurek, R. W., O'Neill, A., and Swinbank, R.: On the motion of air through stratospheric polar vortex, J. Atmos. Sci., 51, 2973–2994, 1994.

Manney, G. L., Zurek, R. W., Lahoz, W. A., Harwood, R. S., Kumer, J. B., Mergenthaler, J., Roche, A. E., O'Neill, A., Swinbank, R., and Waters, J. W.: Lagrangian transport calculations using UARS data. Part I: Passive tracers, J. Atmos. Sci., 52, 3049–3068, 1995.

Manney, G. L., Krüger, K., Sabutis, J. L., Sena, S. A., and Pawson, S.: The remarkable 2003–2004 winter and other recent warm winters in the Arctic stratosphere since the late 1990s, J. Geophys. Res., 110, D04107, doi:10.1029/2004JD005367, 2005.

Manney, G. L., Santee, M. L., Froidevaux, L., Hoppel, K., Livesey, N. J., and Waters, J. W.: EOS MLS observations of ozone loss in the 2004–2005 Arctic winter, Geophys. Res. Lett., 33, L04802, doi:10.1029/2005GL024494, 2006.

Manney, G. L., Daffer, W. H., Zawodny, J. M., et al.: Solar Occultation Satellite Data and Derived Meteorological Products: Sampling Issues and Comparisons with Aura MLS, J. Geophys. Res., 112, D24S50, doi:10.1029/2007JD008709, 2007.

Manney, G. L., Daffer, W. H., Strawbridge, K. B., Walker, K. A., Boone, C. D., Bernath, P. F., Kerzenmacher, T., Schwartz, M. J., Strong, K., Sica, R. J., Krger, K., Pumphrey, H. C., Lambert, A., Santee, M. L., Livesey, N. J., Remsberg, E. E., Mlynczak, M. G., and Russell III, J. R.: The high Arctic in extreme winters: vortex, temperature, and MLS and ACE-FTS trace gas evolution, Atmos. Chem. Phys., 8, 505–522, 2008a, http://www.atmos-chem-phys.net/8/505/2008/.

Manney, G. L., Krueger, K., Pawson, S., Minschwaner, K., Schwartz, M. J., Daffer, W., Livesey, N. J., Mlynczak, M. G., Remsberg, E., Russell, J. M., and Waters, J. W.: The evolution of the stratopause during the 2006 major warming: Satellite Data and Assimilated Meteorological Analyses, J. Geophys. Res., 113, D11115, doi:10.1029/2007JD009097, 2008b.

Medvedev, A. S. and Klaassen, G. P: Realistic Semiannual Oscillation Simulated in a Middle Atmosphere General Circulation Model, Geophys. Res. Lett., 28(4), 733–736, 2001.

Mote, P. W., Rosenlof, K. H., Mclntyre, M. E., Carr, E. S., Gille, J. C., Holton, J. R., Kinnersley, J. S., Pumphrey, H. C., Russell III, J. M., and Waters, J. W.: An atmospheric tape recorder: The imprint of tropical tropopause temperatures on stratospheric water vapor, J. Geophys. Res., 101(D2), 3989–4006, 1996.

Murtagh, D., Frisk, U., Merino, F., et al.: An overview of the Odin atmospheric mission, Can. J. Phys., 80(4), 309–319, 2002.

Plumb, R. A.: Stratospheric transport, J. Meteor. Soc. Japan, 80, 793–809, 2002.

Plumb, R. A., Heres, W., Neu, J. L., Mahowald, N. M., del Corral, J., Toon, G. C., Ray, E., Moore, F., and Andrews, A. E.: Global

tracer modeling during SOLVE: High-latitude descent and mixing, J. Geophys. Res., 107, 8309, doi:10.1029/2001JD001023, 2002 (printed 108(D5), 2003).

Polavarapu, S., Ren, S. Z., Rochon, Y., Sankey, D., Ek, N., Koshyk, J., and Tarasick, D.: Data assimilation with the Canadian middle atmosphere model, Atmos.-Ocean, 43(1), 77–100, 2005.

Pumphrey, H. C., Filipiak, M. J., Livesey, N. J., Schwartz, M. J., Boone, C., Walker, K. A., Bernath, P., Ricaud, P., Barret, B., Clerbaux, C., Jarnot, R. F., Manney, G. L., and Waters, J. W.: Validation of middle-atmosphere carbon monoxide retrievals from MLS on Aura, J. Geophys. Res., 112, D24S38, doi:10.1029/2007JD008723, 2007.

Pumphrey H. C., Boone, C., Walker, K. A., Bernath, P., and Livesey, N. J.:, Tropical tape recorder observed in HCN, Geophys. Res. Lett., 35, L05801, doi:10.1029/2007GL032137, 2008.

Randall, C. E., Harvey, V. L., Singleton, C. S., Bernath, P. F., Boone, C. D., and Kozyra, J. U.: Enhanced NOx in 2006 linked to strong upper stratospheric Arctic vortex, Geophys. Res. Lett., 33, L18811, doi:10.1029/2006GL027160, 2006.

Randel, W. J., Wu, F., Russell III, J. M., Roche, A., and Waters, J. W.: Seasonal Cycles and QBO Variations in Stratospheric CH4 and H2O Observed in UARS HALOE Data, J. Atmos. Sci., 55, 163–185, 1998.

Randel, W. J., Wu, F., Gettelman, A., Russell III, J. M., Zawodny, J. M., and Oltmans, S. J.: Seasonal variation of water vapor in the lower stratosphere observed in Halogen Occultation Experiment data, J. Geophys. Res., 106(13), 14313–14325, 2001.

Randel, W. J., Park, M., Wu, F., and Livesey, N. J.: A large annual cycle in ozone above the tropical tropopause linked to the Brewer-Dobson circulation, J. Atmos. Sci., 64, 4479–4488, 2007.

Ray, E., Holton, J. R., Fishbein, E. F., Froidevaux, L., and Waters, J. W.: The tropical semiannual oscillation in temperature and ozone observed by the MLS, J. Atmos. Sci., 51, 3045–3052, 1994.

Rinsland, C. P., Boone, C., Nassar, R., Walker, K., Bernath, P., McConnell, J. C., and Chiou, L.: Atmospheric Chemistry Experiment (ACE) Arctic stratospheric measurements of NOx during February and March 2004: Impact of intense solar flares, Geophys. Res. Lett., 32, L16S05, doi:10.1029/2005GL022425, 2005.

Russell III, J. M., Gordley, L. L., Park, J. H., Drayson, S. R., Hesketh, W. D., Cicerone, R. J., Tuck, A. F., Frederick, J. E., Harries, J. E., and Crutzen, P. J.: The Halogen Occultation Experiment, J. Geosphys. Res., 98(D6), 10777–10797, 1993.

Schoeberl, M. R., Luo, M., and Rosenfield, J. E.: An analysis of the Antarctic Halogen Occultation Experiment trace gas observations, J. Geophys. Res., 100(D3), 5159–5172, 1995.

Schoeberl, M. R., Duncan, B. N., Douglass, A. R., Waters, J., Livesey, N., Read, W., and Filipiak, M.: The carbon monoxide tape recorder, Geophys. Res. Lett., 33, L12811, doi:10.1029/2006GL026178, 2006.

Schoeberl, M. R., Douglass, A. R., Newman, P. A., Lait, L. R., Lary, D., Waters, J., Livesey, N., Froidevaux, L., Lambert, A., Read, W., Filipiak, M. J., and Pumphrey, H. C.: QBO and Annual Cycle Variations in Tropical Lower Stratosphere Trace Gases from HALOE and Aura MLS Observations, J. Geophys. Res. 113, D05301, doi:10.1029/2007JD008678, 2008.

Shepherd, T. G.: The middle atmosphere, J. Atmos. Solar-Terr. Phys., 62, 1587–1601, 2000.

Shepherd, T. G. and Jonsson, A. I.: On the attribution of stratospheric ozone and temperature changes to changes in ozone-depleting substances and well-mixed greenhouse gases, Atmos. Chem. Phys., 8, 1435–1444, 2008,
http://www.atmos-chem-phys.net/8/1435/2008/.

Shepherd, T. G.: Transport in the middle atmosphere, J. Meteor. Soc. Japan, 85B, 165–191, 2007.

Siskind, D. E., Eckermann, S. D., Coy, L., McCormack, J. P., and Randall, C. E.: On recent interannual variability of the Arctic winter mesosphere: Implications for tracer descent, Geophys. Res. Lett., 34, L09806, doi:10.1029/2007GL029293, 2007.

Strong, K., Wolff, M. A., Kerzenmacher, T. E., et al.: Validation of ACE-FTS $N_2O$ measurements, Atmos. Chem. Phys., 8, 4759–4786, 2008,
http://www.atmos-chem-phys.net/8/4759/2008/.

Tian, W., Chipperfield, M. P., Gray, L. J., and Zawodny, J. M.: Quasi-biennial oscillation and tracer distributions in a coupled chemistry-climate model, J. Geophys. Res., 111, D20301, doi:10.1029/2005JD006871, 2006.

Urban, J., Lautié, N., Le Flochmoën, E., et al.: Odin/SMR limb observations of stratospheric trace gases: Validation of $N_2O$, J. Geophys. Res., 110, D09301, doi:10.1029/2004JD005394, 2005.

Urban, J., Murtagh, D. P., Lautié, N., et al.: Odin/SMR Limb Observations of Trace Gases in the Polar Lower Stratosphere during 2004–2005, Proc. ESA First Atmospheric Science Conference, 8–12 May 2006, Frascati, Italy, edited by: Lacoste, H., ESA-SP-628 Noordwijk: European Space Agency, ISBN/ISSN: ISBN-92-9092-939-1, ISSN-1609-042X, 2006.

Waters, J. W., Froidevaux, L., Harwood, R. S., et al.: The Earth Observing System Microwave Limb Sounder (EOS MLS) on the Aura satellite, IEEE Trans. Geosci. Remote Sensing, 44(5), 1075–1092, 2006.

World Meteorological Organization (WMO): Scientific Assessment of Ozone Depletion: 2002, Global Ozone Research and Monitoring Project, Report No. 47, Geneva, 2003.

World Meteorological Organization (WMO): Scientific Assessment of Ozone Depletion: 2006, Global Ozone Research and Monitoring Project, Report No. 50, Geneva, 2007.

Zhang, X. C.: The semi-annual oscillation in the middle atmosphere: A comparison of CMAM with HALOE measurements, M.Sc. dissertation, York University, Canada, 2002.